A new measurement of the Kaonic Helium L-lines with SIDDHARTA-2 at DAΦNE

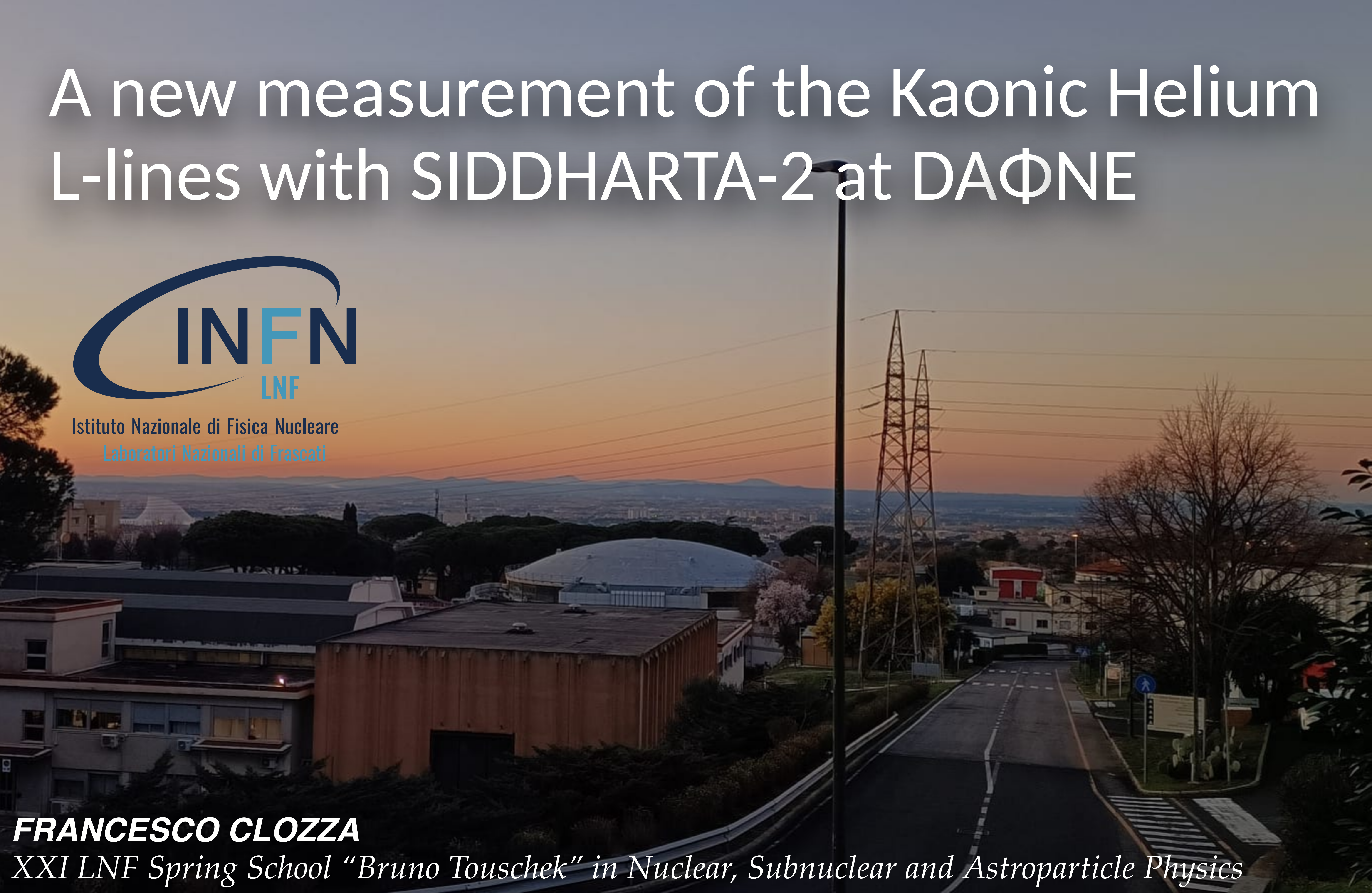

INFN
LNF
Istituto Nazionale di Fisica Nucleare
Laboratori Nazionali di Frascati

FRANCESCO CLOZZA

XXI LNF Spring School "Bruno Touschek" in Nuclear, Subnuclear and Astroparticle Physics

Physics of light kaonic atoms

On the Disintegration of Negative Mesons

M. CONVERSI, E. PANCINI, AND O. PICCIONI*

Centro di Fisica Nucleare del C. N. R. Istituto di Fisica dell'Università di Roma, Italia

December 21, 1946

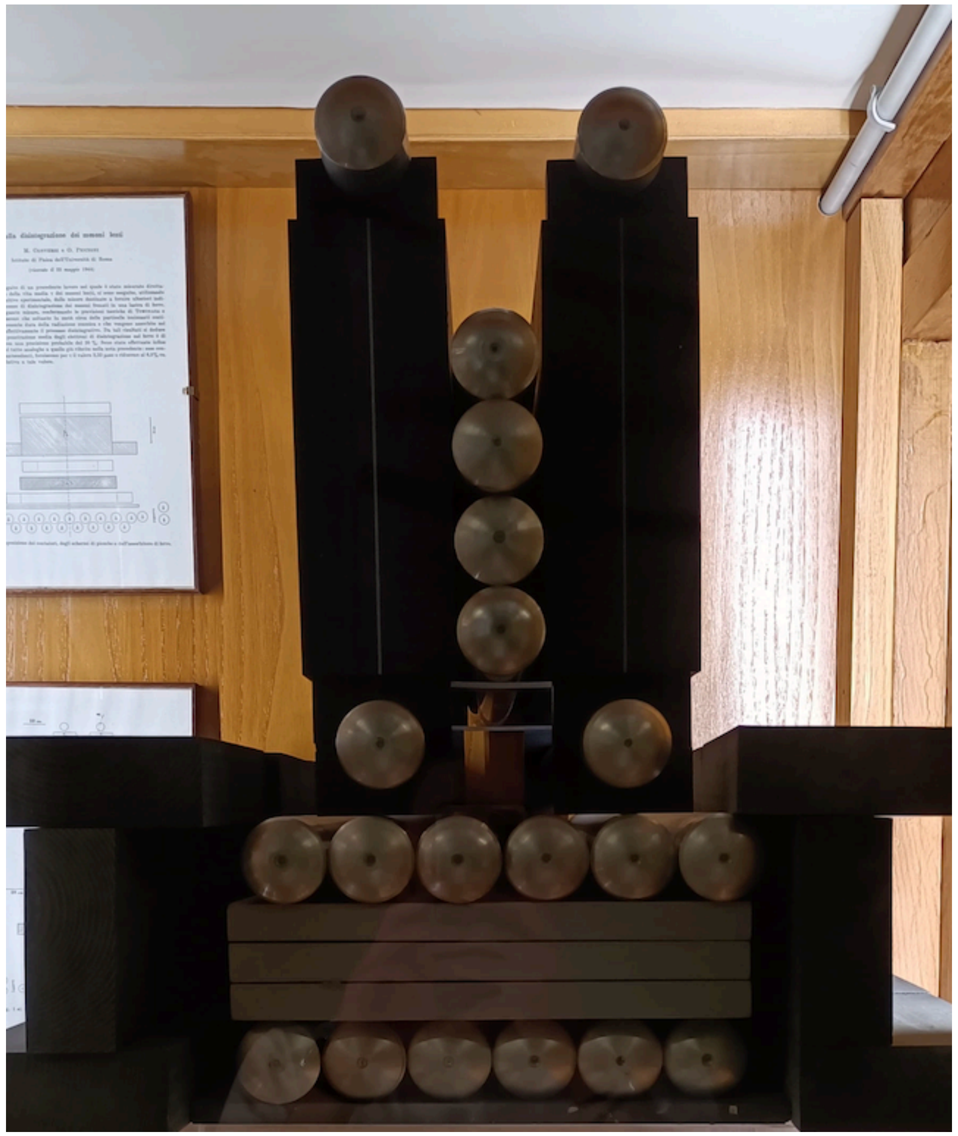

- Predicted in the '40s (Tomonaga and Araki, 1940; Conversi, Pancini, and Piccioni 1945, 1947)
- Exotic Atoms: atoms in which a negatively charged particle replaces an electron in the atomic orbits
- Study of hadronic atoms to probe the strong interaction between the hadron and the nucleus at vanishing relative energy
- Kaonic atoms offers a unique way of directly probing the non-perturbative QCD with strangeness

Physics of light kaonic atoms

- K^- slowed down and stopped inside a target
- Atomic capture followed by cascade process
- K^- captured in an highly excited state n
- Emission of radiation following the de-excitation

$$n \sim \sqrt{\frac{\mu}{m_e}} n_e$$

$n \sim 28$ K-^{4}He & K-D

$n \sim 25$ K-H

μ system's reduced mass

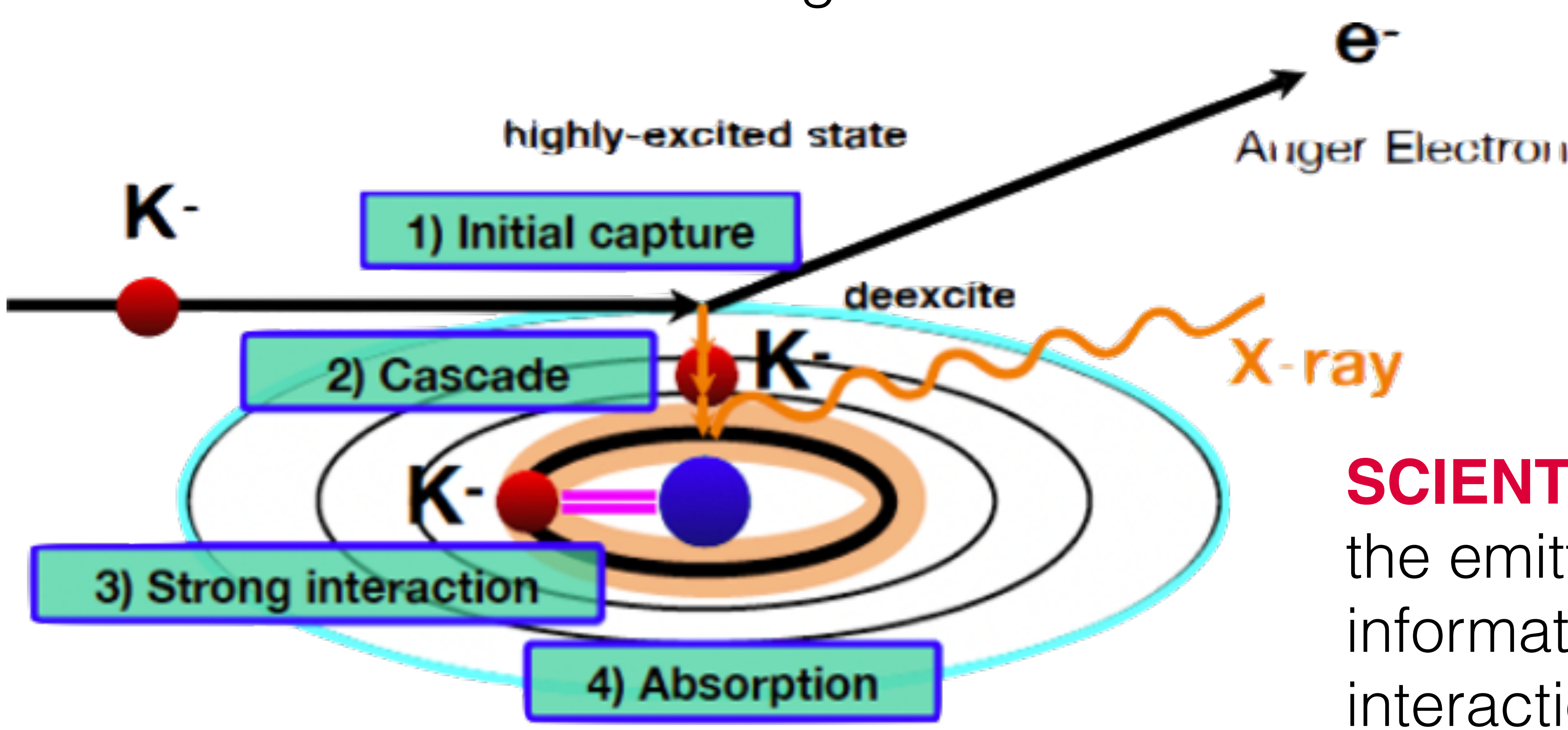

SCIENTIFIC GOAL: measure the emitted X-Rays to extract information on the K-N interaction

Why kaonic helium-4?

- Kaonic deuterium $2p \rightarrow 1s$ transition exhibits a drastically low X-ray yield

- Challenging measure

- An accurate and thorough characterisation and optimisation of the experimental apparatus is mandatory:
  1. Characterisation of the Silicon Drift Detectorts (SDDs) used to perform X-ray spectroscopy
  2. Optimisation of the degrader to maximise the number of kaons stopped

- **Kaonic helium-4** $3d \rightarrow 2p\ (L_\alpha)$ transition exhibits an X-ray yield ~ 100 greater

- Best candidate to fulfil this purpose

Kaonic Helium Puzzle

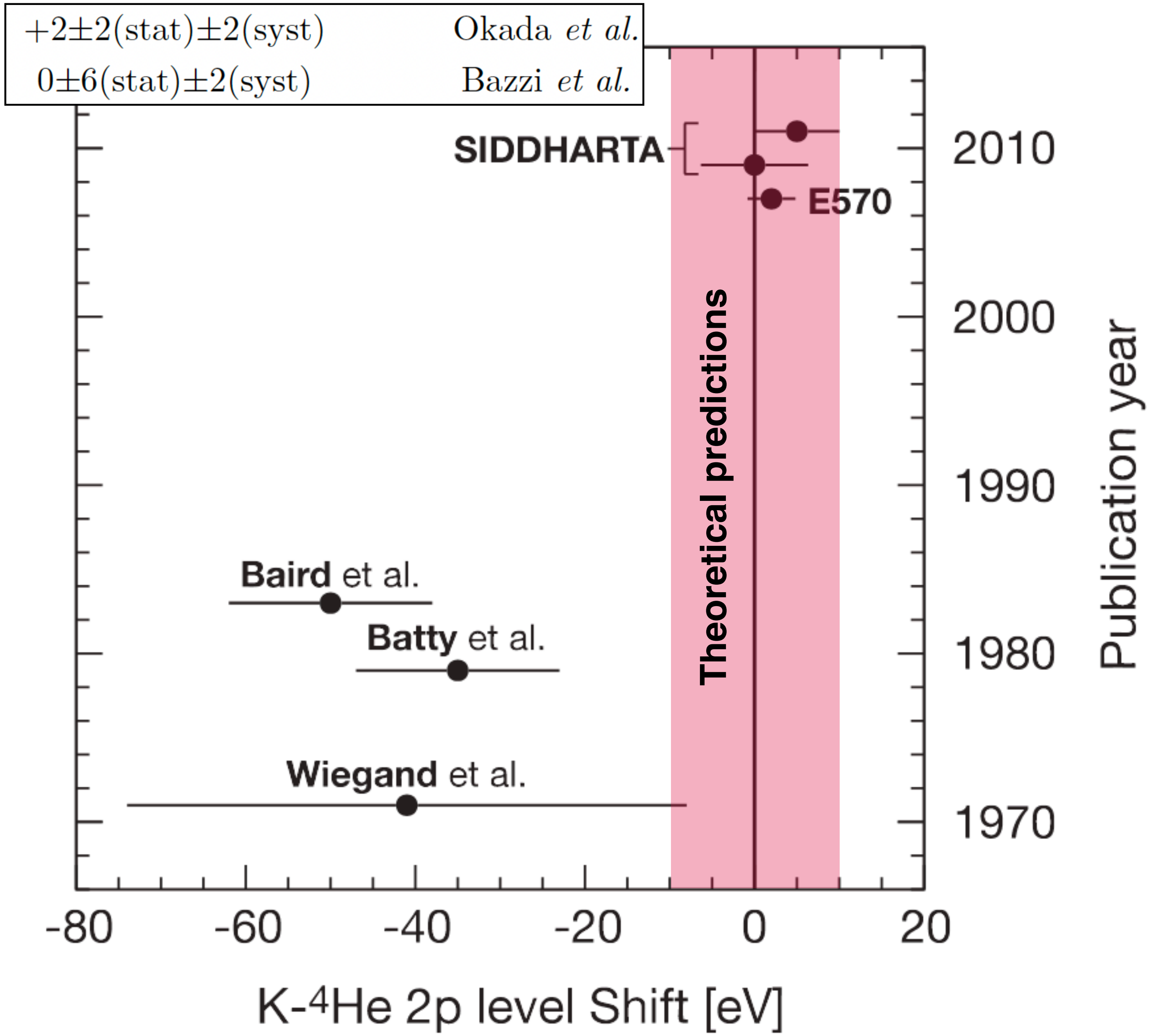

- Need of more accurate measurements to investigate any small shift
- The characterisation campaign of the new SIDDHARTA-2 experimental apparatus is a unique opportunity to perform a new and more accurate measurement of the kaonic helium-4 $3d \rightarrow 2p$ transition

Experimental Setup

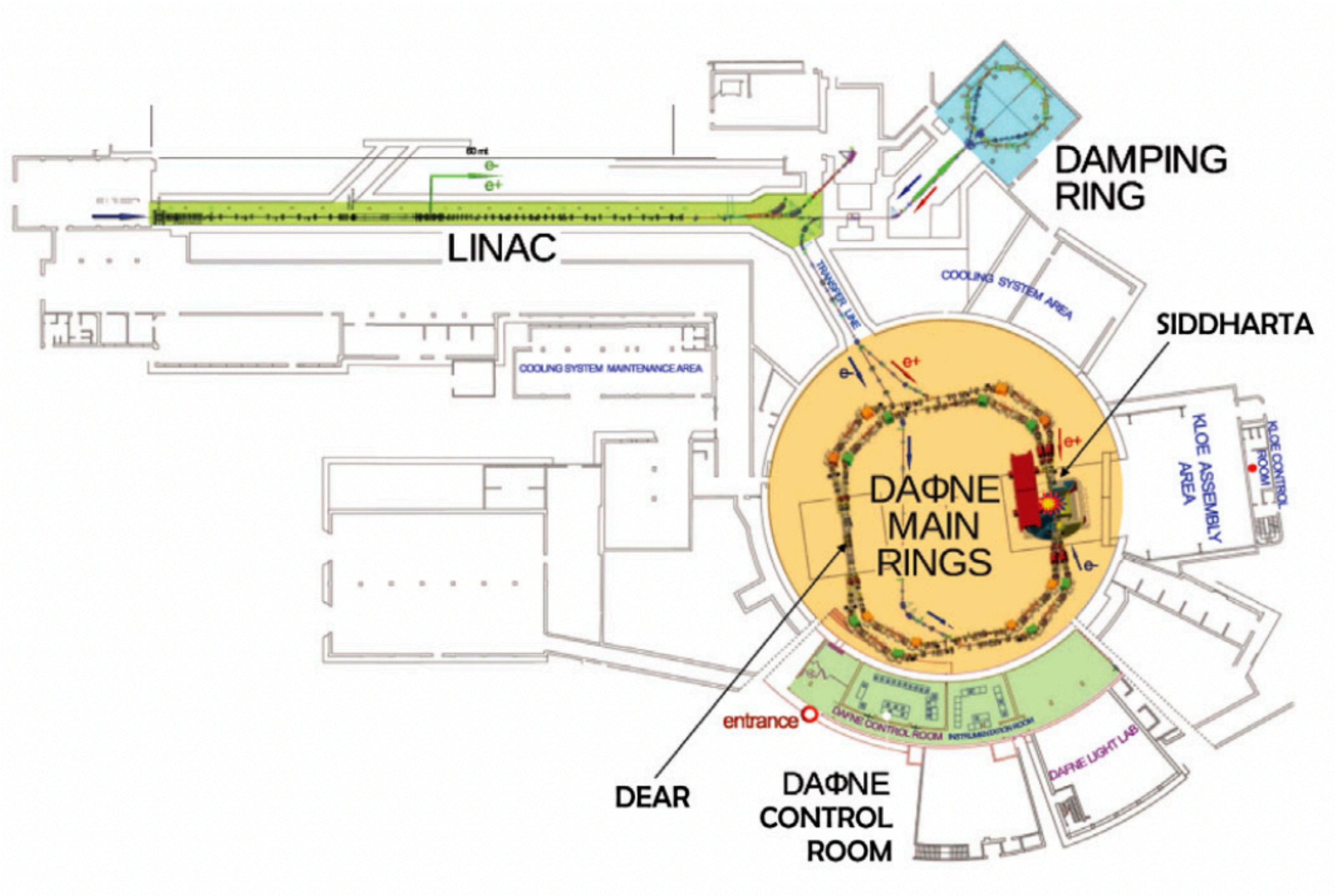

- SIDDHARTA-2 experiment installed on the Interaction Point (IP) of DAΦNE
- e^+e^- collider working at a center of mass energy of the ϕ meson mass (1.02 GeV/c^2)
- Decay to K^+K^- pairs with a BR of 48.9%
- **Kaon momentum 127MeV/c**
- Not (much) relativistic $\beta \sim 0.25$, $\beta\gamma \sim 0.26$

Experimental Setup

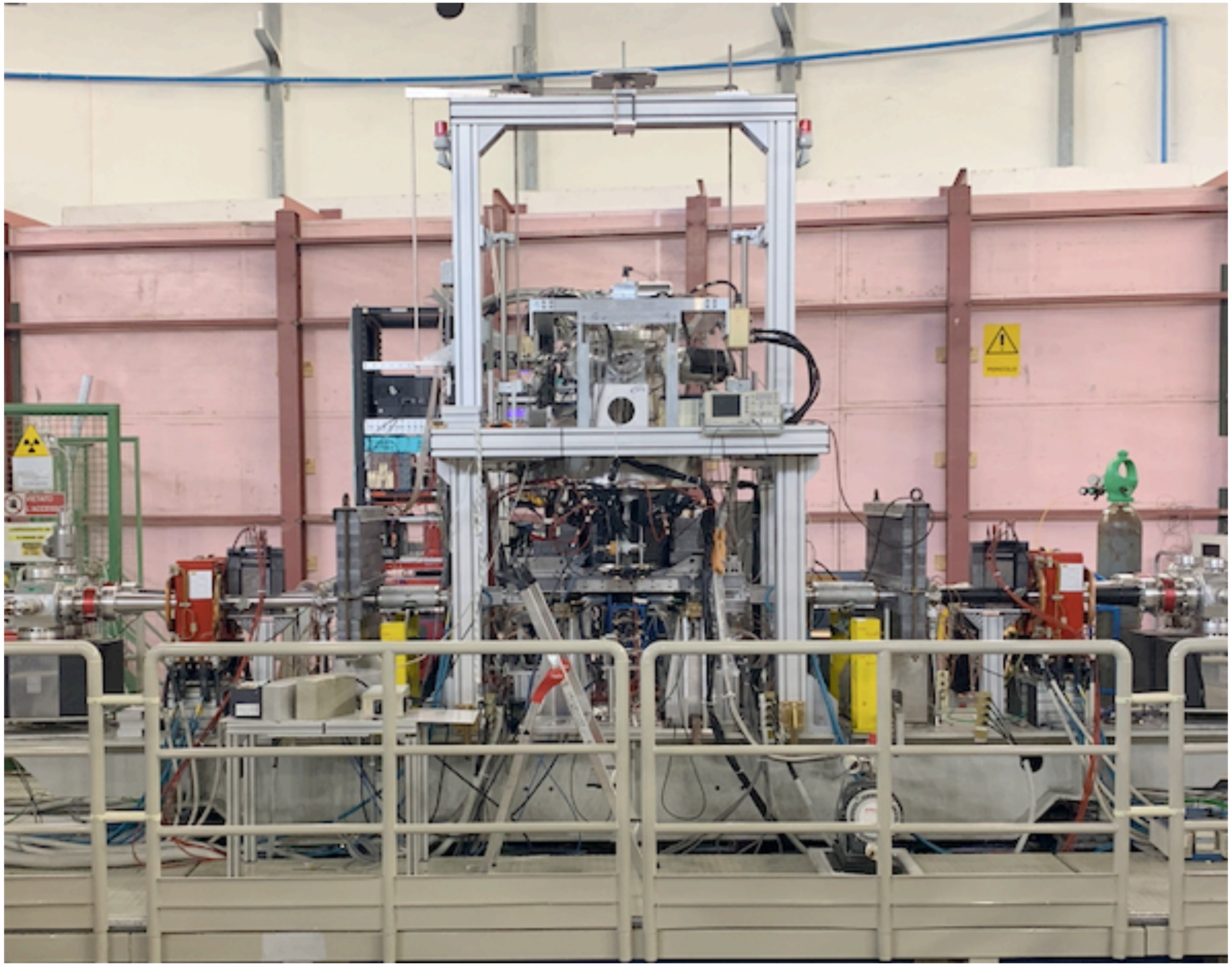

Final SIDDHARTA-2 apparatus installed in DAΦNE in September 2022

Experimental Setup

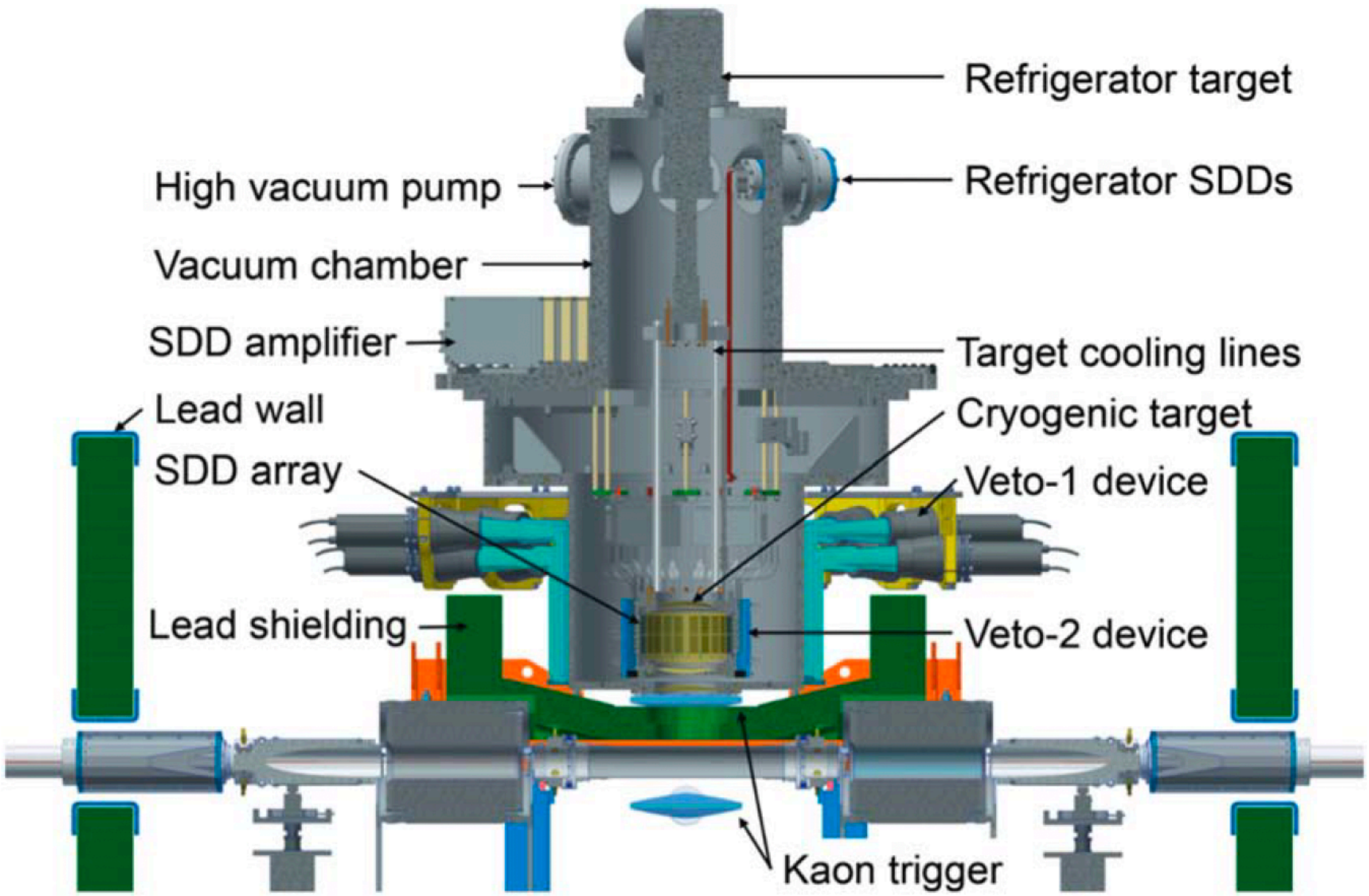

- Beam pipe
- Cylindrical vacuum chamber
- Cryogenic target cell
- Kaon trigger
- 384 X-Ray detectors (SDDs)
- Mylar degrader
- Luminosity monitor
- Veto Systems

Experimental Setup: kaon trigger

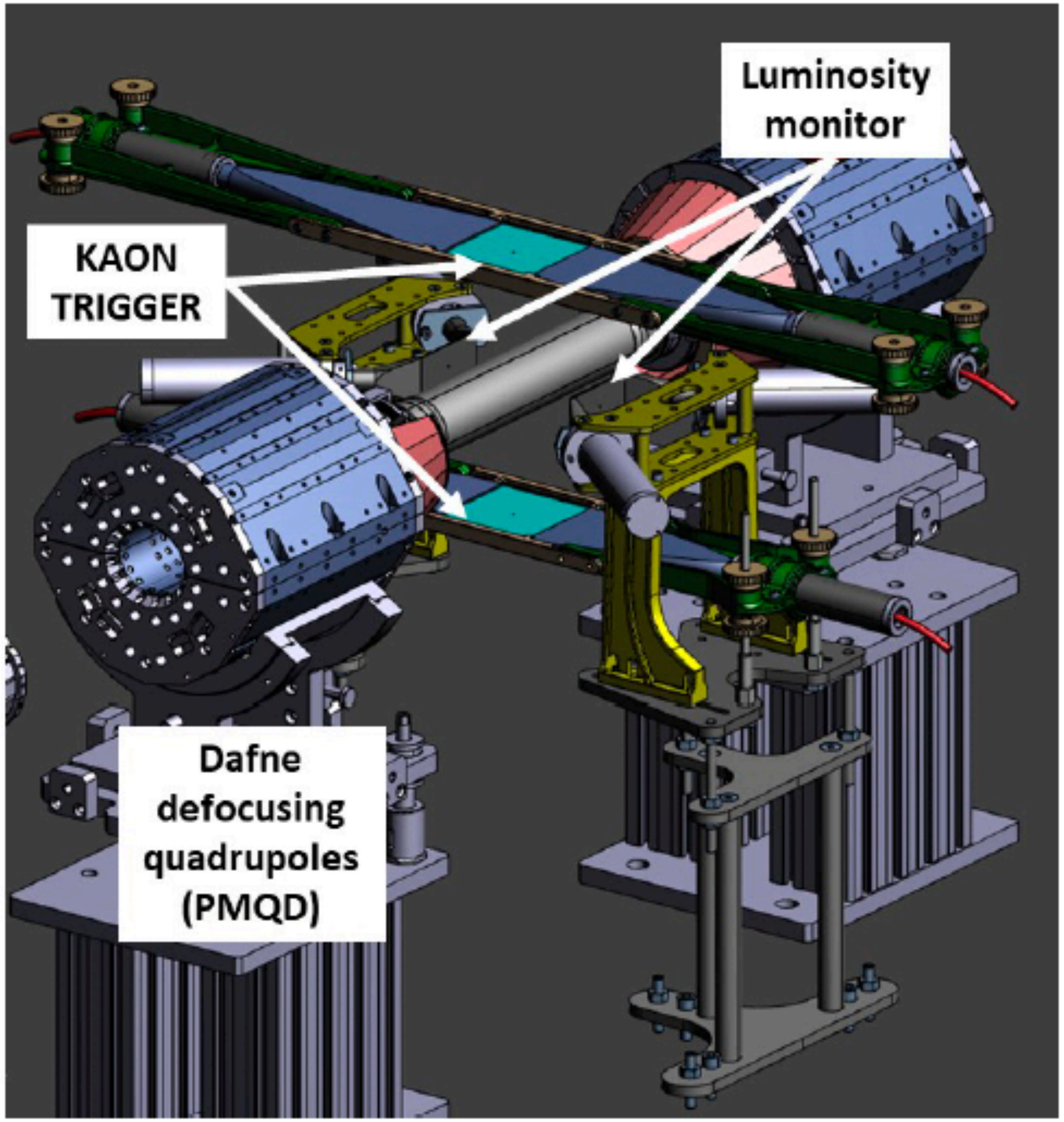

- Pair of plastic scintillators above and below the IP
- Read by two PMTs each
- Selection of kaons as coincidence between the scintillators
- Suppression of asynchronous background related to particle losses from e^+e^- beams due to Touschek effect
- MIPs-induced triggers suppressed with Time-of-Flight TOF signatures

Experimental Setup: SDDs

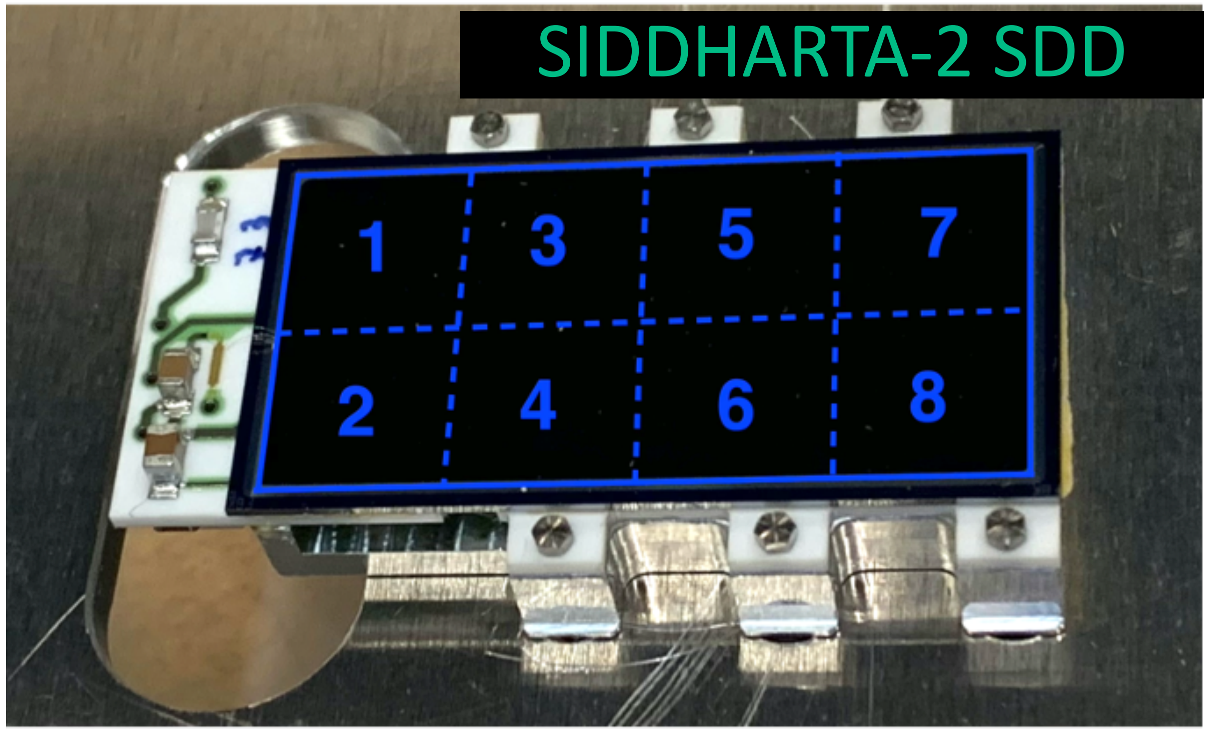

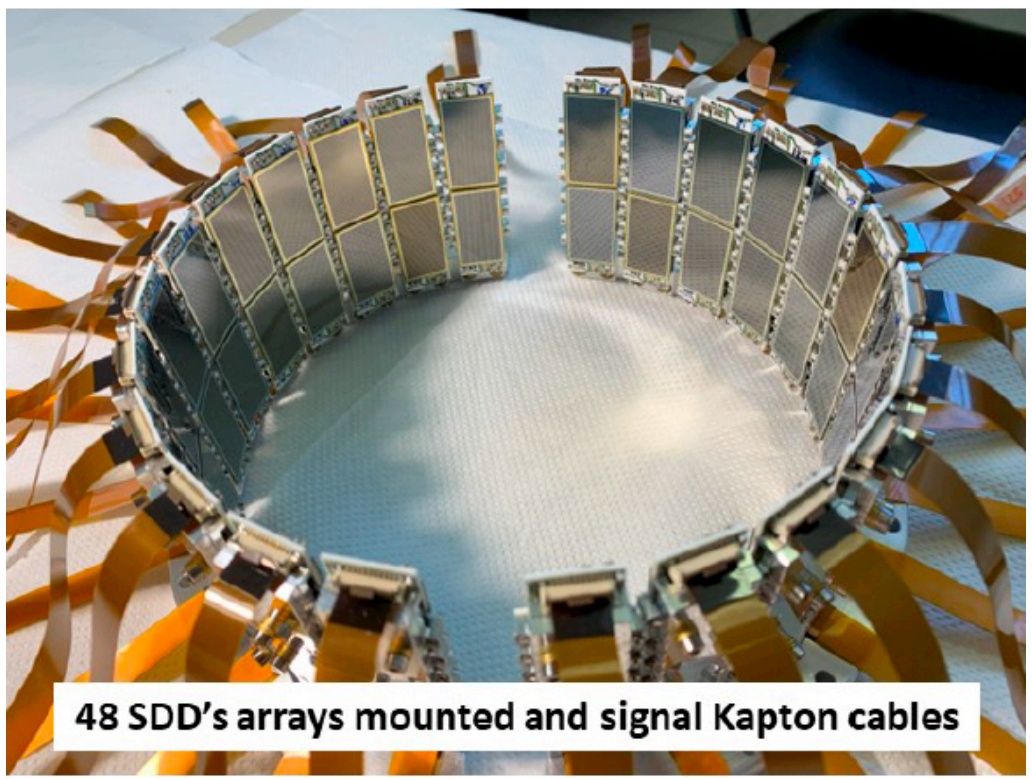

- SDD cells: 8x8mm^2 active area
- 450µm thick silicon bulk: it allows a ~100% detection efficiency for 5-12keV X-rays (~7keV region of interest for kaonic deuterium)
- SDD cells packed in 2x4 array (total active area of 5.12cm^2)
- Silicon wafer glued on alumina ceramic carrier

Experimental Setup: SDDs calibration

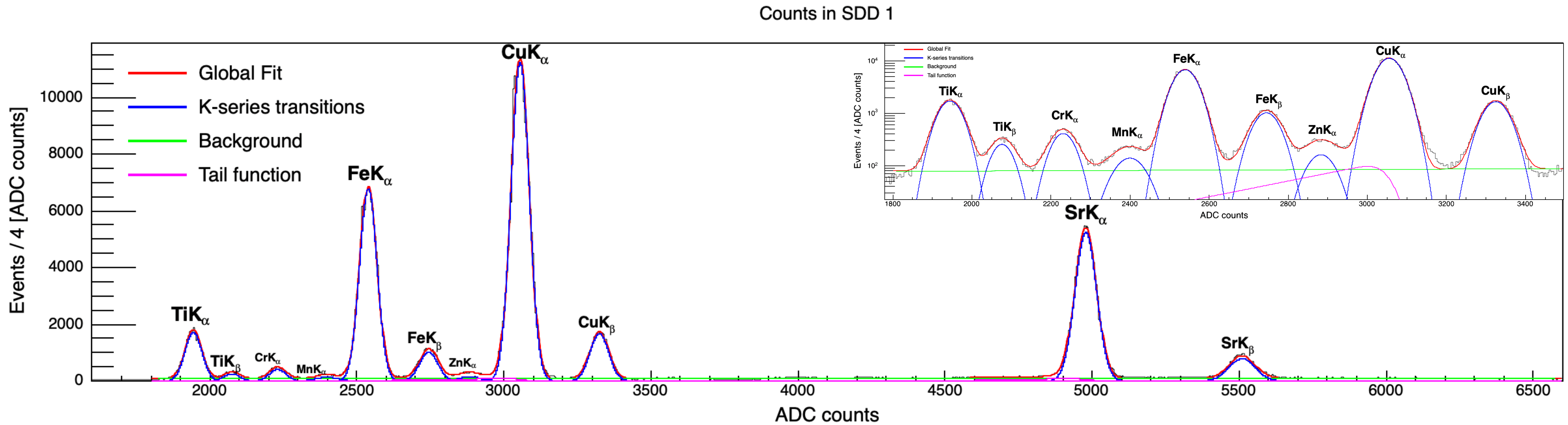

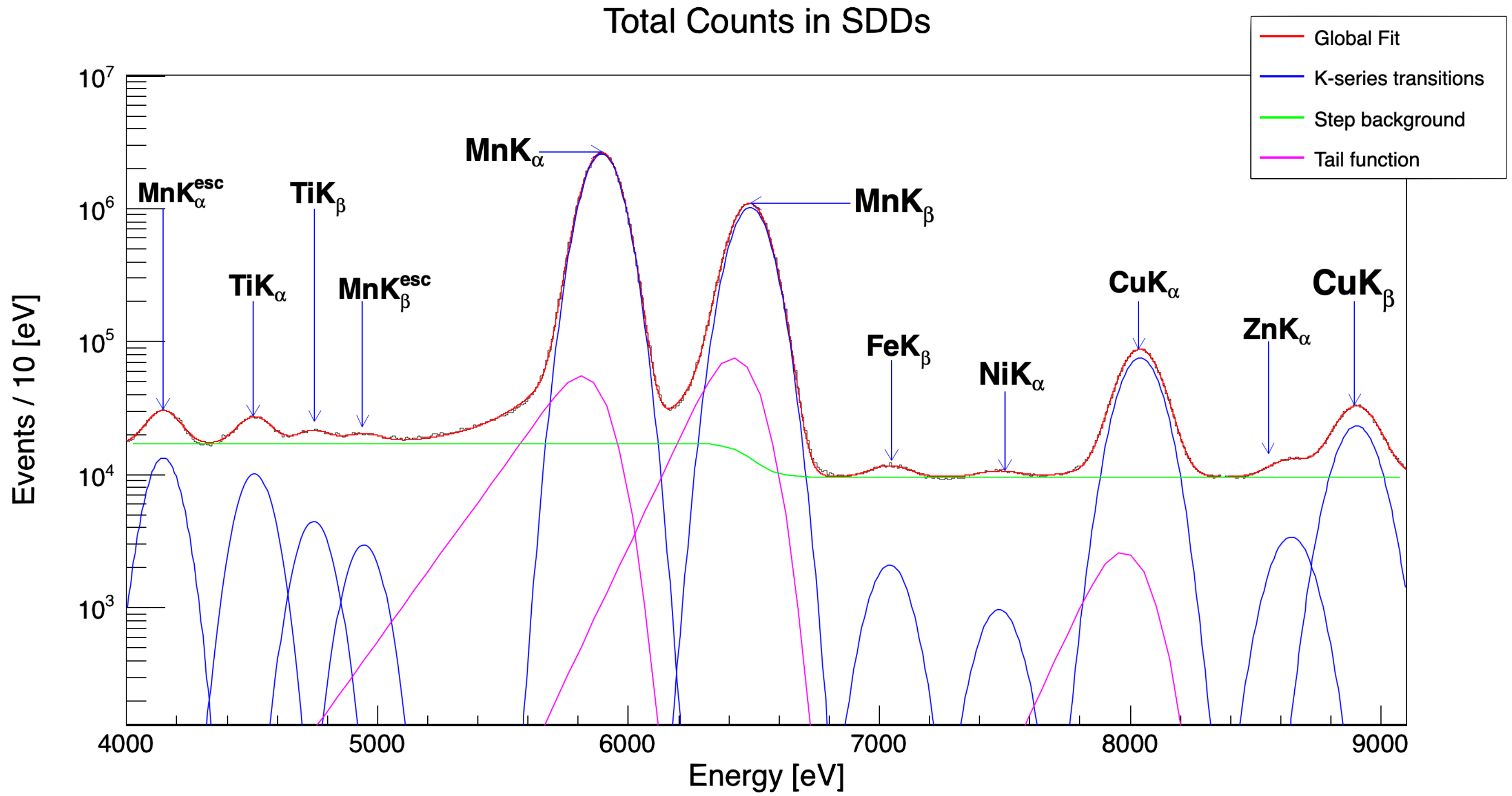

- SDDs energy response characterized in a controlled environment
- Calibration of 321 SDDs in the DAΦNE hall
- Systematic errors for the final measurement $(\varepsilon_{2p}, \Gamma_{2p})$

Data selection

- Inclusive spectrum for a kaolic helium-4 measurement at a density of 1.88 g/L and a total integrated luminosity of $\sim 31\,\mathrm{pb}^{-1}$ made between April and May 2023
- High background hinders the observation of the kaonic helium lines

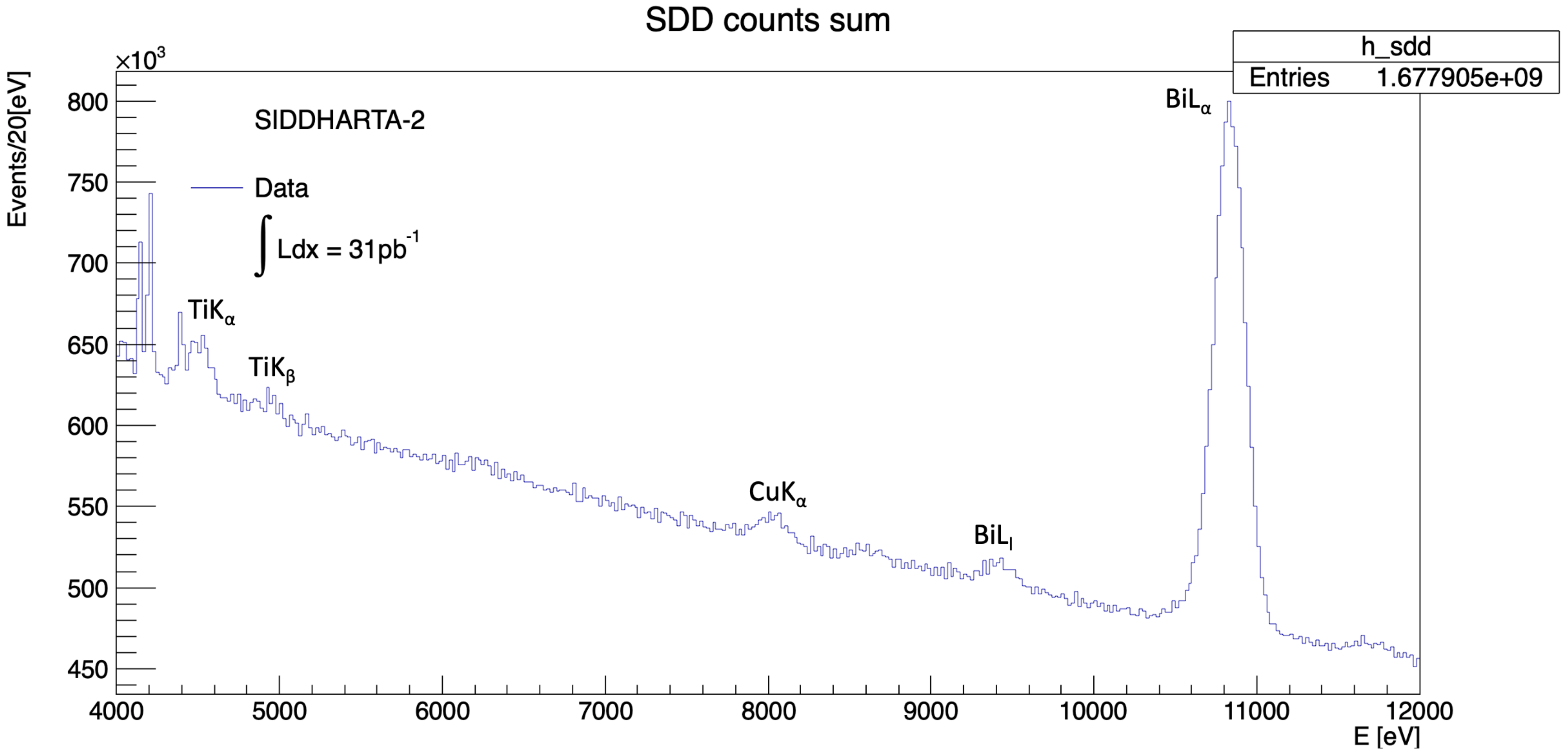

Data selection: kaon trigger

- Kaon trigger (KT) used to:
  1. suppress the asynchronous background due to beam losses, 5μs time window in coincidence with a KT signal
  2. reduce MIPs-induced triggers with TOF signatures

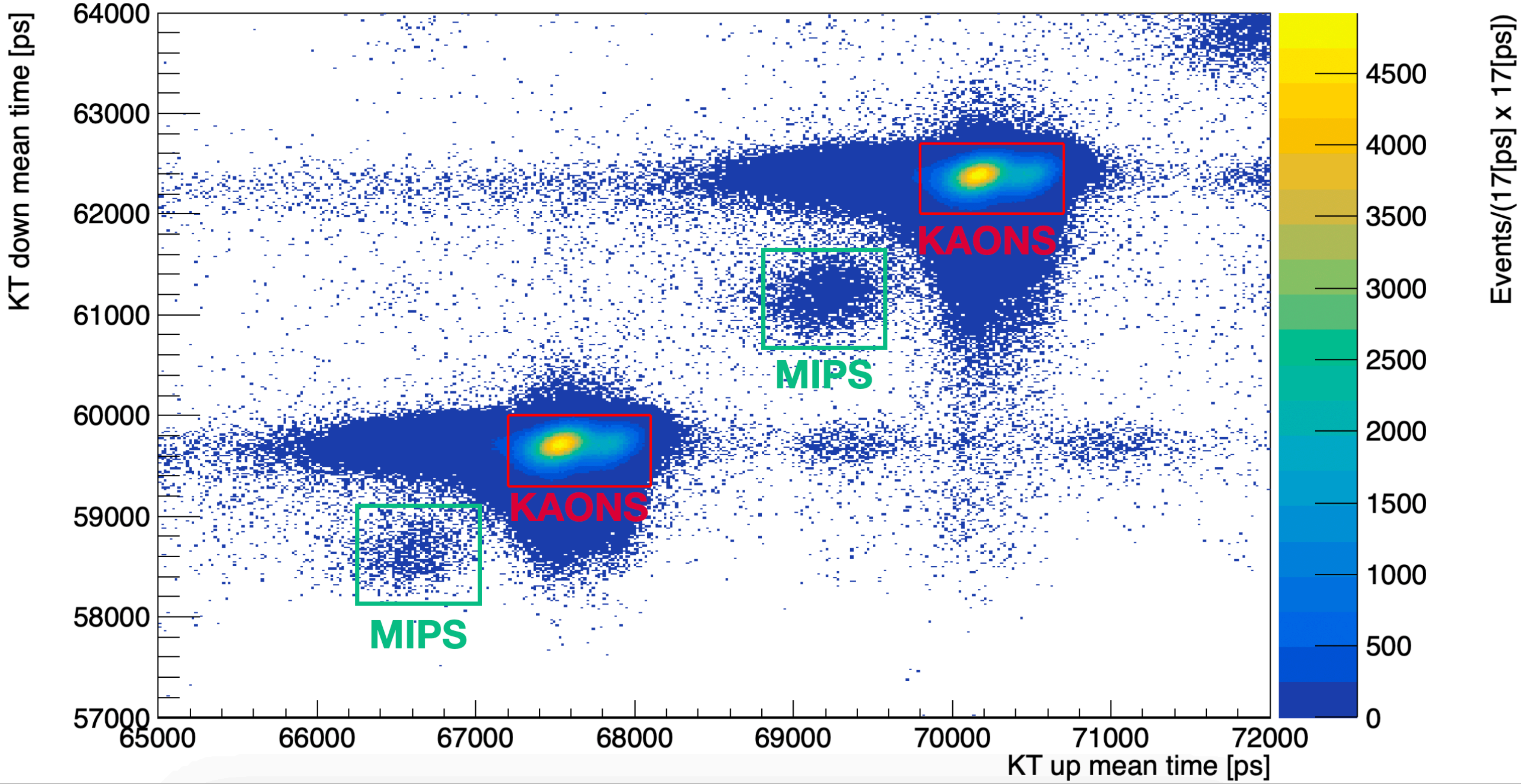

Data selection: drift time

- Time difference between KT signal and X-ray detection
- Events inside the lines are related to hits on the SDDs in coincidence with the KT signals
- Time resolution extracted: FWHM $= (507.60 \pm 0.47)$ ns

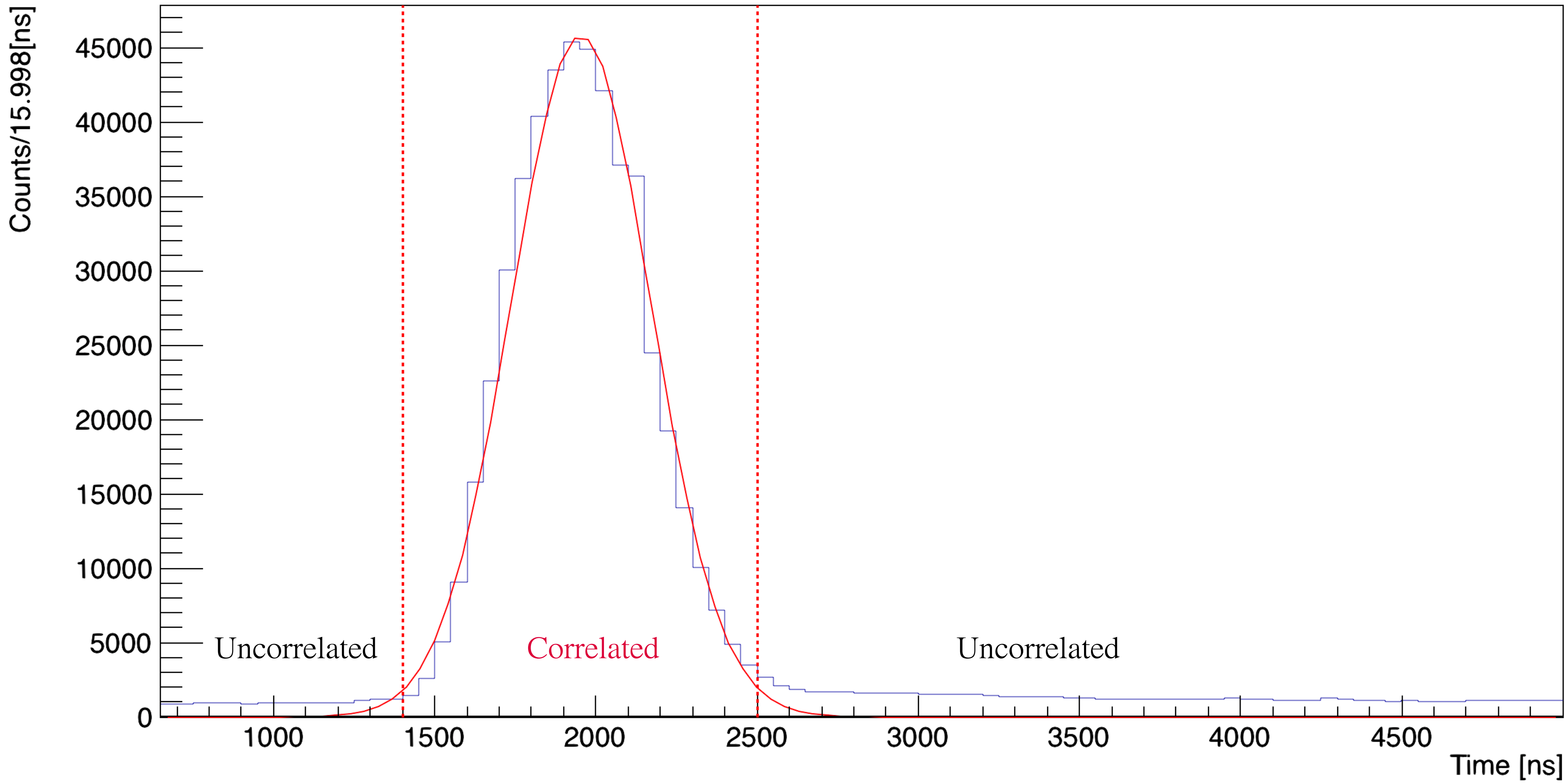

Data selection: rejection factor

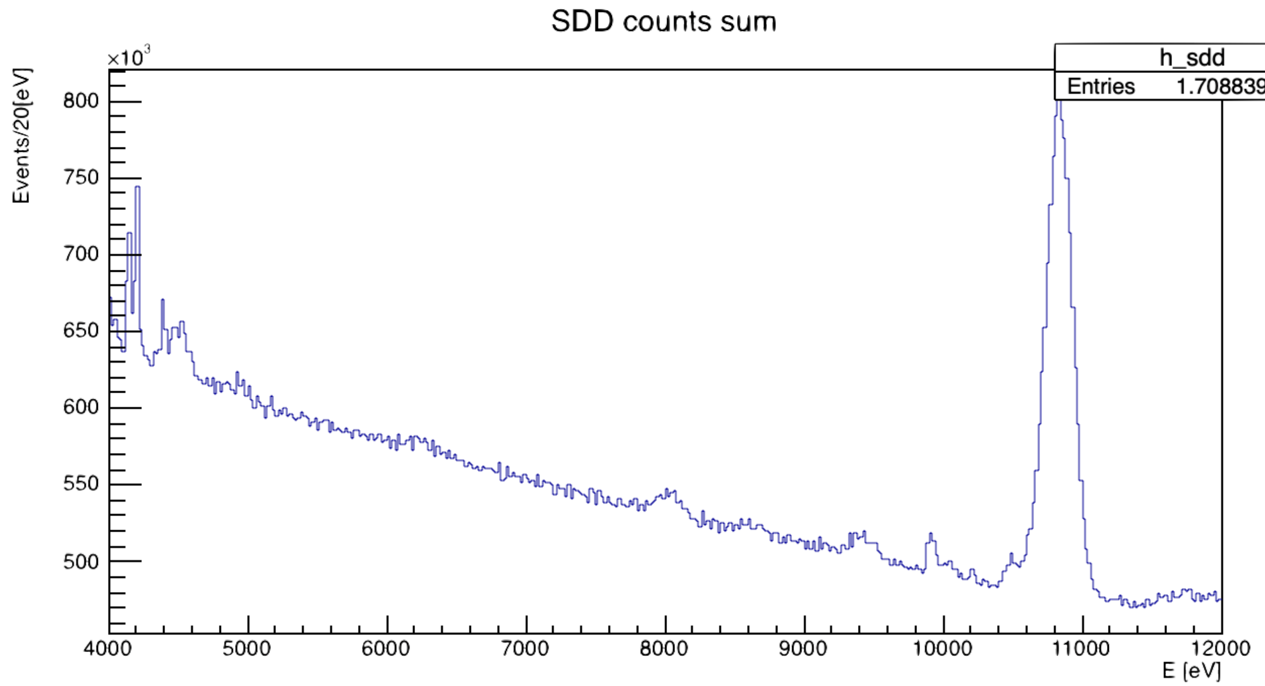

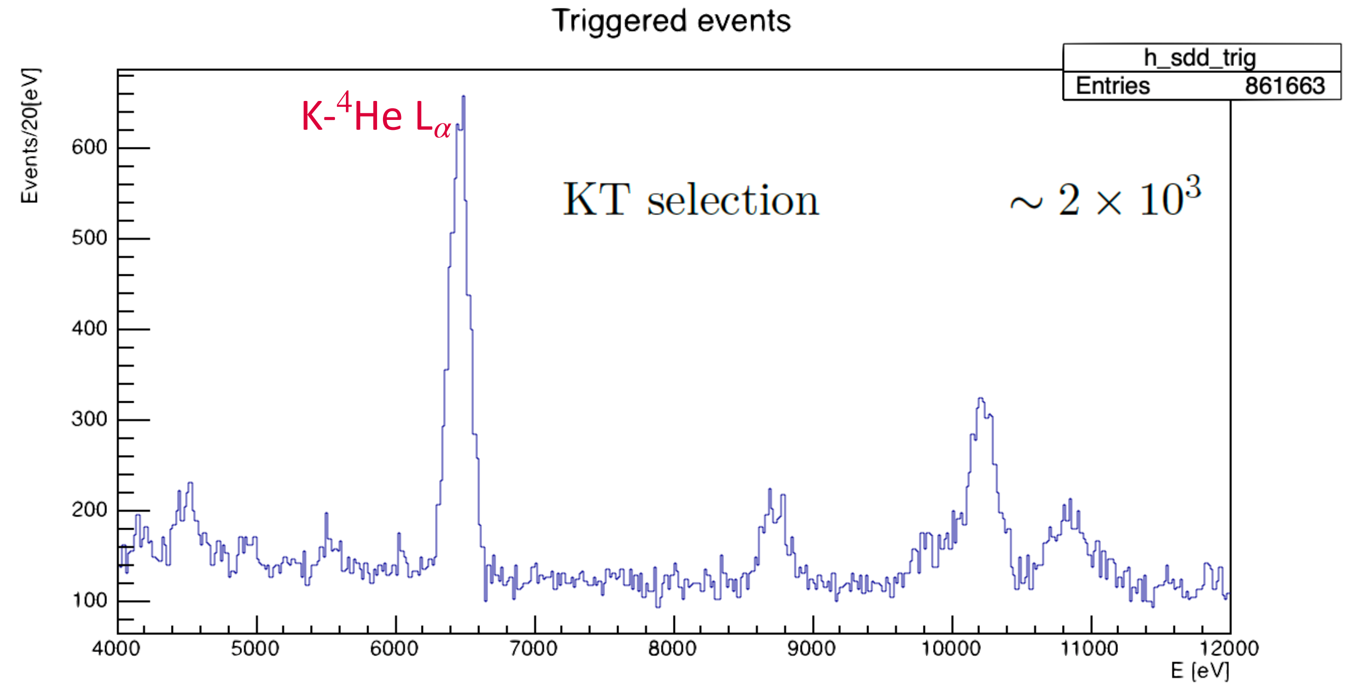

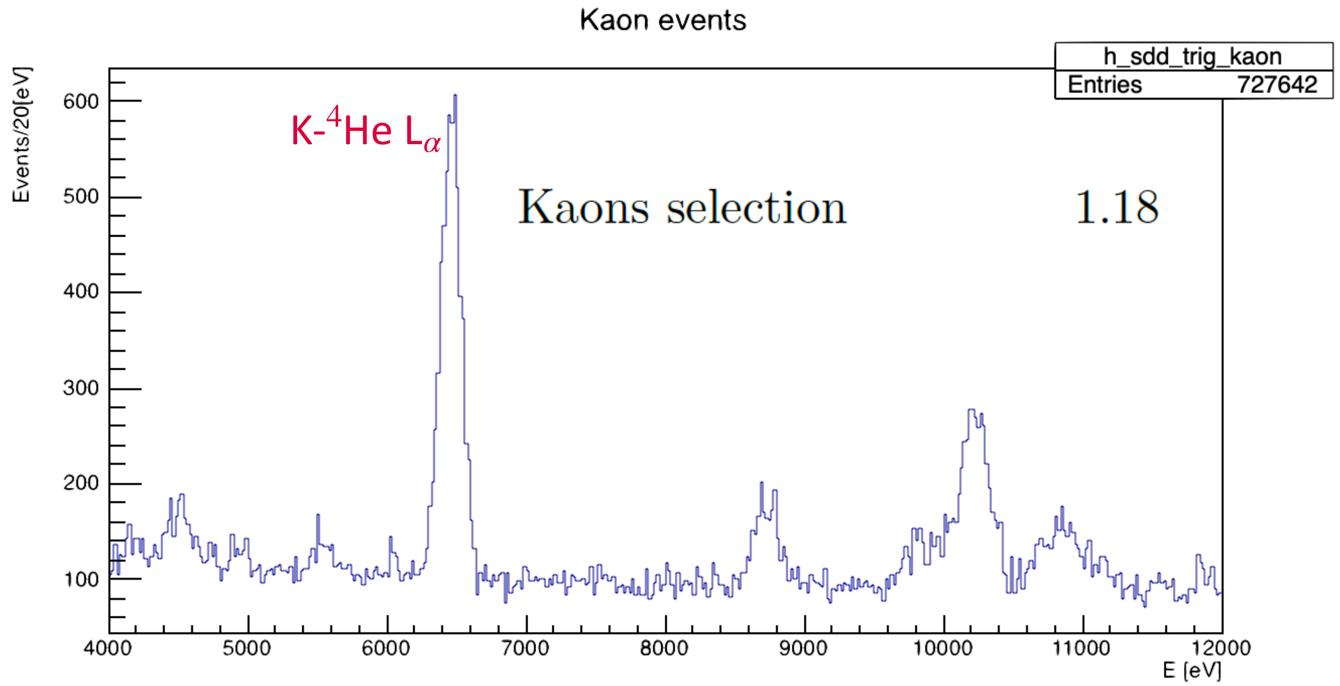

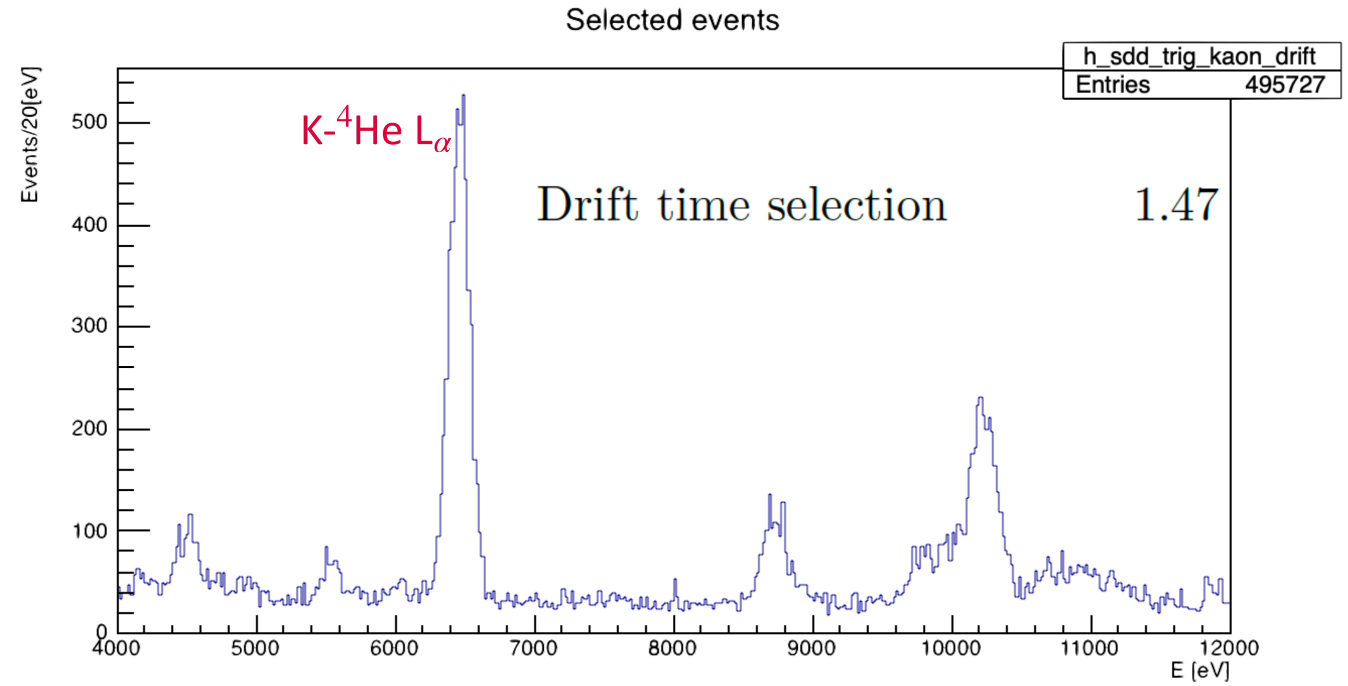

total rejection factor $\sim 10^3$

Kaonic Helium L-series measurement

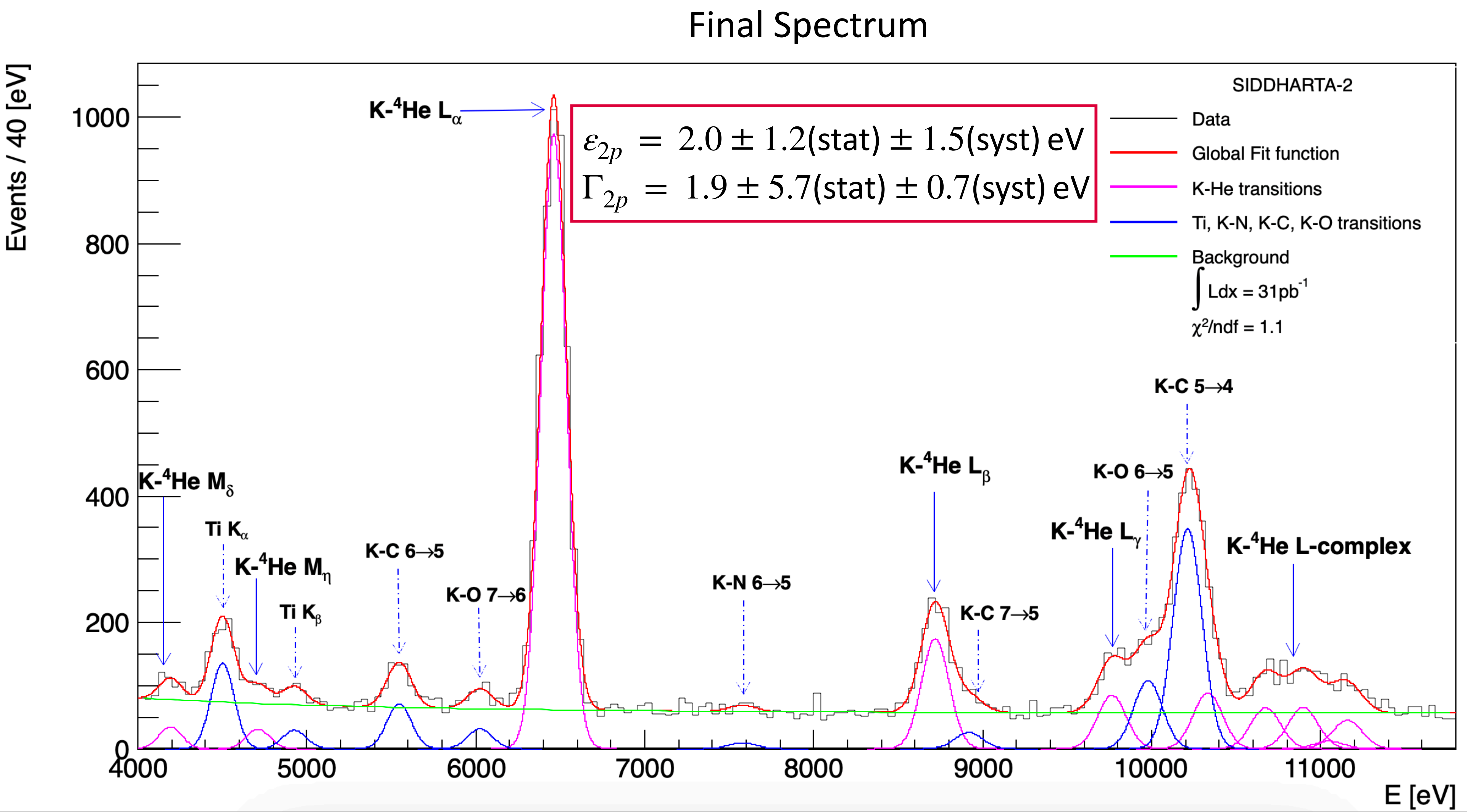

Kaonic Helium L-series measurement

$$\varepsilon_{2p} = 2.0 \pm 1.2(\text{stat}) \pm 1.5(\text{syst})\ \text{eV}$$

This work, with the **new SIDDHARTA-2 apparatus**

Vs

SIDDHARTA measurement (2009)

$$\varepsilon_{2p} = 0 \pm 6(\text{stat}) \pm 2(\text{syst})\ \text{eV}$$

Bazzi, M. et al. Kaonic helium-4 x-ray measurement in SIDDHARTA. Physics Letters B 681, 310–314 (2009).

Enhancement of almost a **factor 6** in the statistical error

Conclusions

- The SIDDHARTA-2 experiment will perform the first ever measurement of the shift and width induced by the strong interaction on the $1s$ level of Kaonic Deuterium

- The performance of the new apparatus make it the **strongest candidate** to perform the kaonic deuterium measurement

- The new measurement of the Kaonic Helium $3d \rightarrow 2p$ transition is consistent with the hypothesis of null shift and width of the $2p$ energy level

- This work delivered **a new and more accurate measurement** of the $3d \rightarrow 2p$ transition of kaonic helium-4

- This result has been published, DOI: https://doi.org/10.3390/condmat9010016

Thank you for your attention

INFN
LNF
Istituto Nazionale di Fisica Nucleare
Laboratori Nazionali di Frascati

FRANCESCO CLOZZA

XXI LNF Spring School "Bruno Touschek" in Nuclear, Subnuclear and Astroparticle Physics

BACKUP

BACKUP

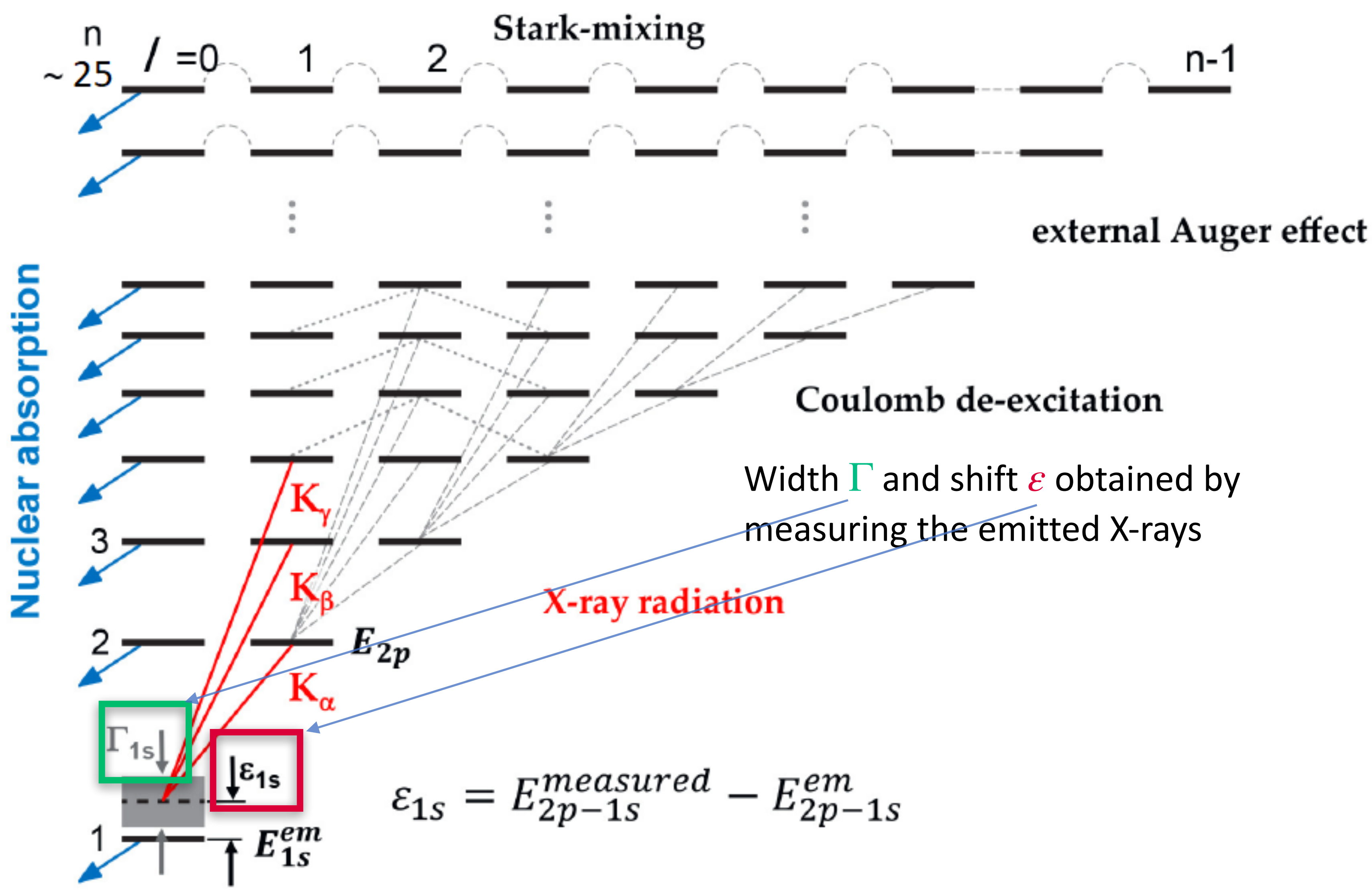

$$\varepsilon_{1s} = E^{measured}_{2p-1s} - E^{em}_{2p-1s}$$

- Detected X-Rays carry information about the (strong) interaction
- Broadening (Γ) and shift (ε) of the energy level induced by the strong interaction
- **Scientific goal:** performing the first measurement of kaonic deuterium X-ray transition to the fundamental level to extract ε_{1s} and Γ_{1s}

BACKUP

- Antikaon-nucleon **scattering lengths** $(a_{\bar{K}N})$ related to these observables

$$\epsilon_{1s}^{H} + \frac{i}{2}\Gamma_{1s}^{H} = 2\alpha^3\mu^2 a_{\bar{K}p}\left[1 - 2\alpha\mu(ln\alpha - 1)a_{\bar{K}p} + \ldots\right]$$

fine structure constant (α) — reduced mass (μ)

Meißner, U.-G., Raha, U. & Rusetsky, A. Spectrum and decays of kaonic hydrogen. The European Physical Journal C-Particles and Fields 35, 349–357 (2004).

$$\lim_{k\to 0}\sigma_e = 4\pi a^2$$

elastic cross section (σ_e)

Landau, L. D. & Lifshitz, E. M. Quantum Mechanics: non-relativistic theory, vol. 3 (Elsevier, 2013).

- Combined analysis of kaonic hydrogen and kaonic deuterium to extract the isospin-dependent antikaon-nucleon scattering lengths
- Kaonic hydrogen measured by the SIDDHARTA experiment in 2009
- Lack of a kaonic deuterium measurement

BACKUP

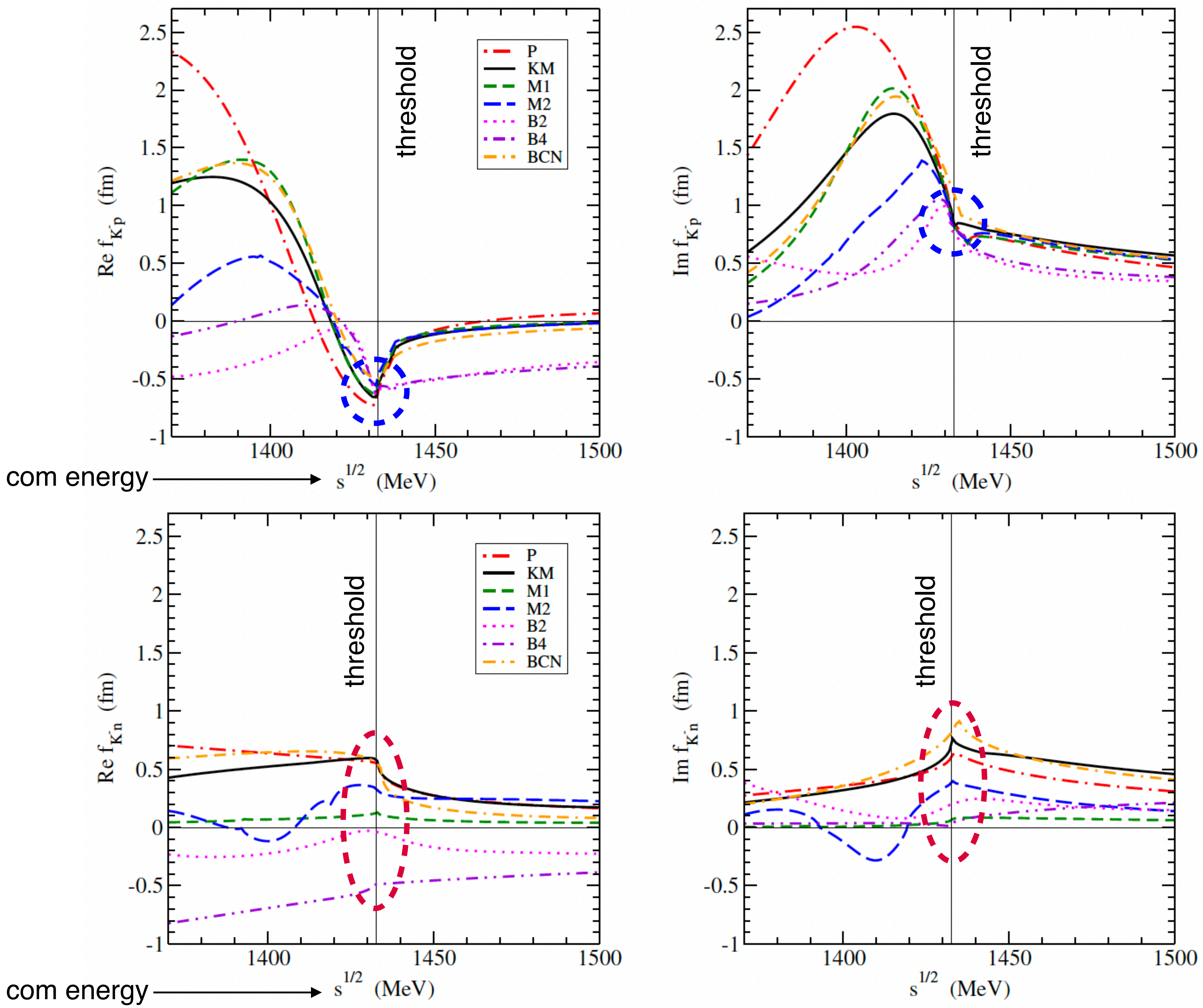

- Theoretical models in good agreement $K^{-}p$ low momentum scattering amplitude
- Theoretical models for the $K^{-}n$ low momentum scattering amplitude highly spread

Óbertová, J., Friedman, E., Mareš, J. & Ramos, À. On K–nuclear interaction, K–nuclear quasibound states and K-atoms. In EPJ Web of Conferences, vol. 271, 07003 (EDP Sciences, 2022).

BACKUP

The $\bar{K}p$ scattering length is connected to the $\bar{K}N$ isospin-dependent scattering lengths a_I, with $I = (0, 1)$, via the relation:

$$a_{\bar{K}p} = \frac{1}{2}(a_0 + a_1) \ . \tag{1.8}$$

The individual isoscalar (a_0) and isovector (a_1) scattering lengths can be obtained by measuring kaonic deuterium, which provides information on a different combination of a_0 and a_1:

$$a_{\bar{K}n} = a_1 \ , \tag{1.9}$$

$$a_{\bar{K}d} = \frac{4\,[m_N + m_K]}{2m_N + m_K} Q + C \ , \tag{1.10}$$

where:

$$Q = \frac{1}{2}\left[a_{\bar{K}p} + a_{\bar{K}n}\right] = \frac{1}{4}\left[a_0 + 3a_1\right] \ . \tag{1.11}$$

BACKUP

$$d\sigma = |f(\theta)|^2\, do. \qquad (123,4)$$

Questa grandezza ha le dimensioni di un'area e si chiama *sezione efficace* (o semplicemente *sezione*) di diffusione entro l'angolo solido do. Ponendo $d0 = 2\pi$ sen $\theta\, d\theta$, otteniamo la sezione d'urto

...

$$d\sigma = 2\pi \,\text{sen}\,\theta\, |f(\theta)|^2\, d\theta \qquad (123,5)$$

per la diffusione nell'intervallo di angoli fra θ e $\theta + d\theta$.

...

In seguito, sarà opportuno usare anche *le ampiezze* di diffusione *parziali* f_l, che determineremo come i coefficienti dello sviluppo

$$f(\theta) = \sum_l (2l+1) f_l P_l(\cos\theta). \qquad (123,14)$$

...

e noi arriviamo alla conclusione che nel caso limite di energie piccole si ha

$$f_l \backsim k^{2l}. \qquad (132,8)$$

In tal modo, tutte le ampiezze parziali con $l \neq 0$ risultano piccole rispetto all'ampiezza di diffusione con $l = 0$ (o, come si dice, di *diffusione s*). Trascurando le ampiezze parziali, abbiamo per l'ampiezza totale

...

$$f(\theta) \approx f_0 = \frac{\delta_0}{k} = \frac{c_2}{c_1} \equiv -\alpha, \qquad (132,9)$$

cosicché $d\sigma = \alpha^2\, do$, e la sezione totale è

$$\sigma = 4\pi\alpha^2. \qquad (132,10)$$

Landau, L. D. & Lifshitz, E. M. Quantum Mechanics: non-relativistic theory, vol. 3 (Elsevier, 2013).

BACKUP

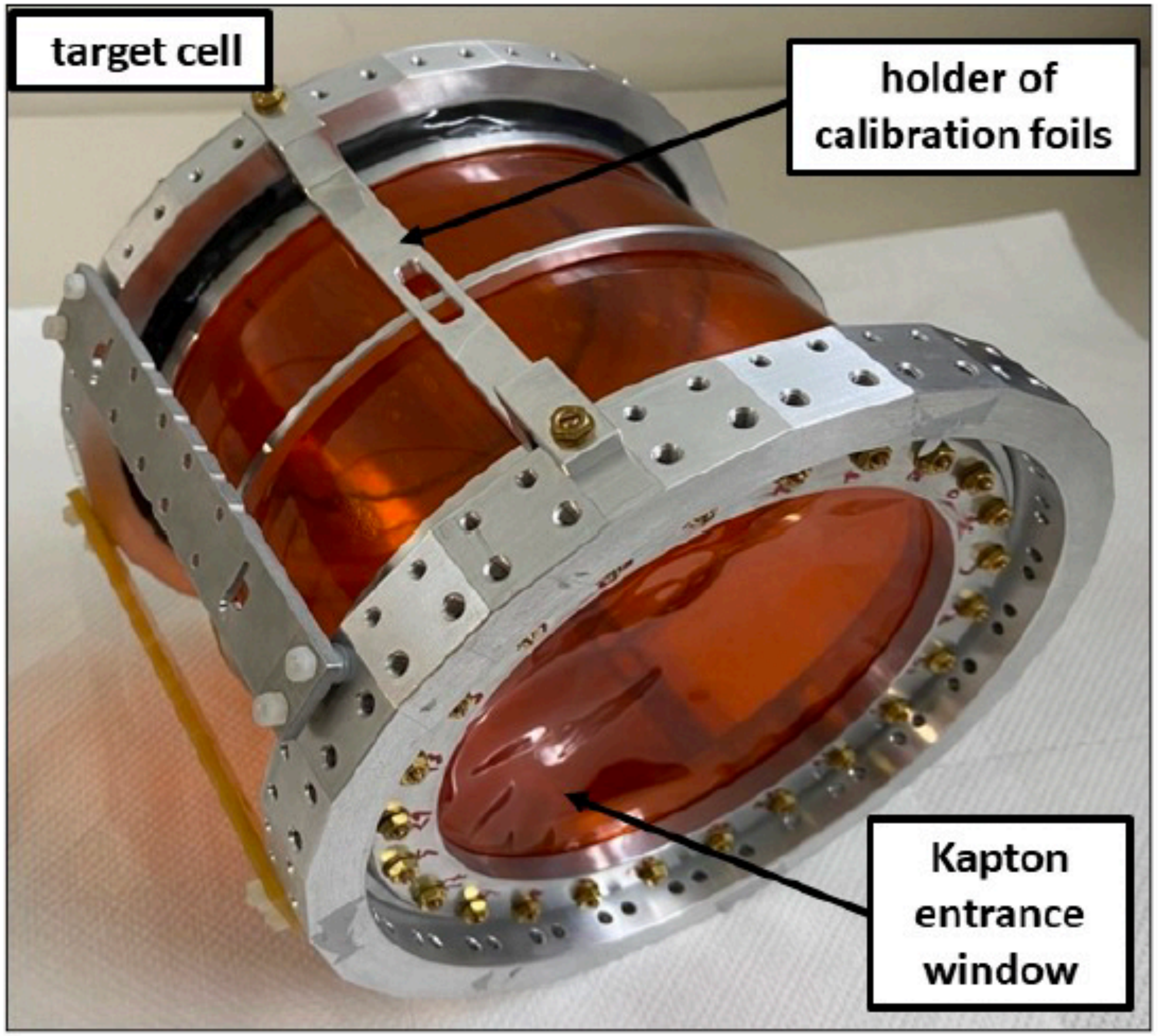

- Cylindrical volume (144mm diameter x 125mm height)
- Side walls made of two layers of 75μm kapton ($C_{22}H_{10}N_2O_5$)
- Reinforcement structure of high purity aluminum
- 125μm thick kapton entrance window
- 100μm thick titanium top roof
- **Gaseous target**
- Target cell kept between 20-30K with a closed-cycle helium refrigeration system

BACKUP

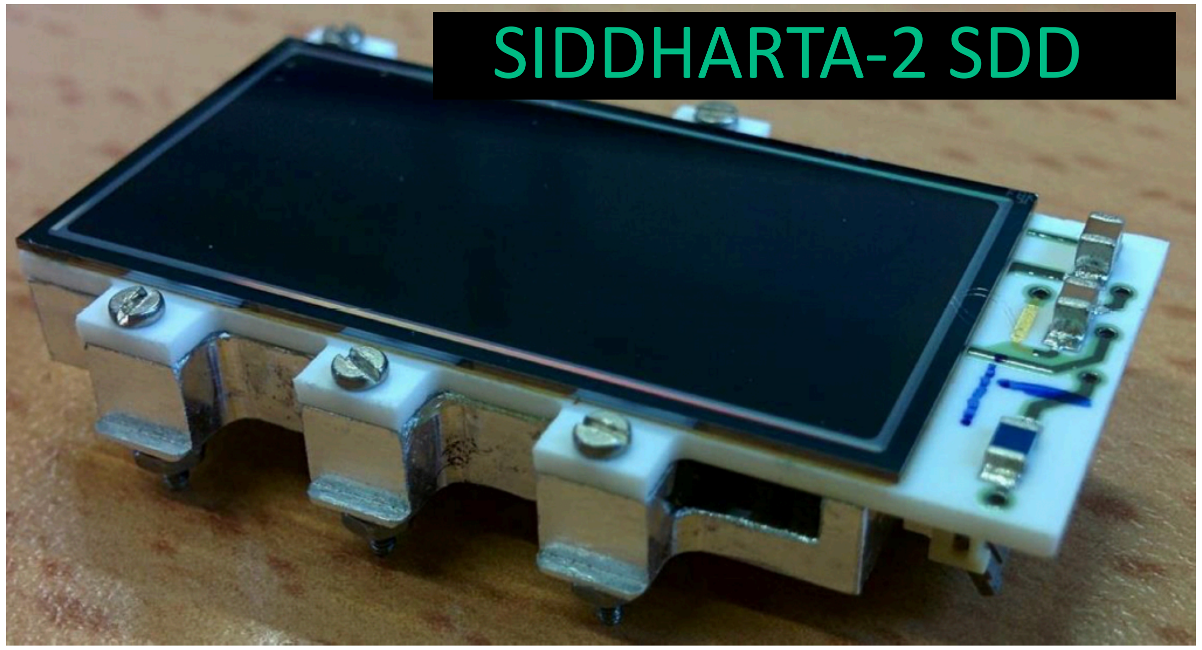

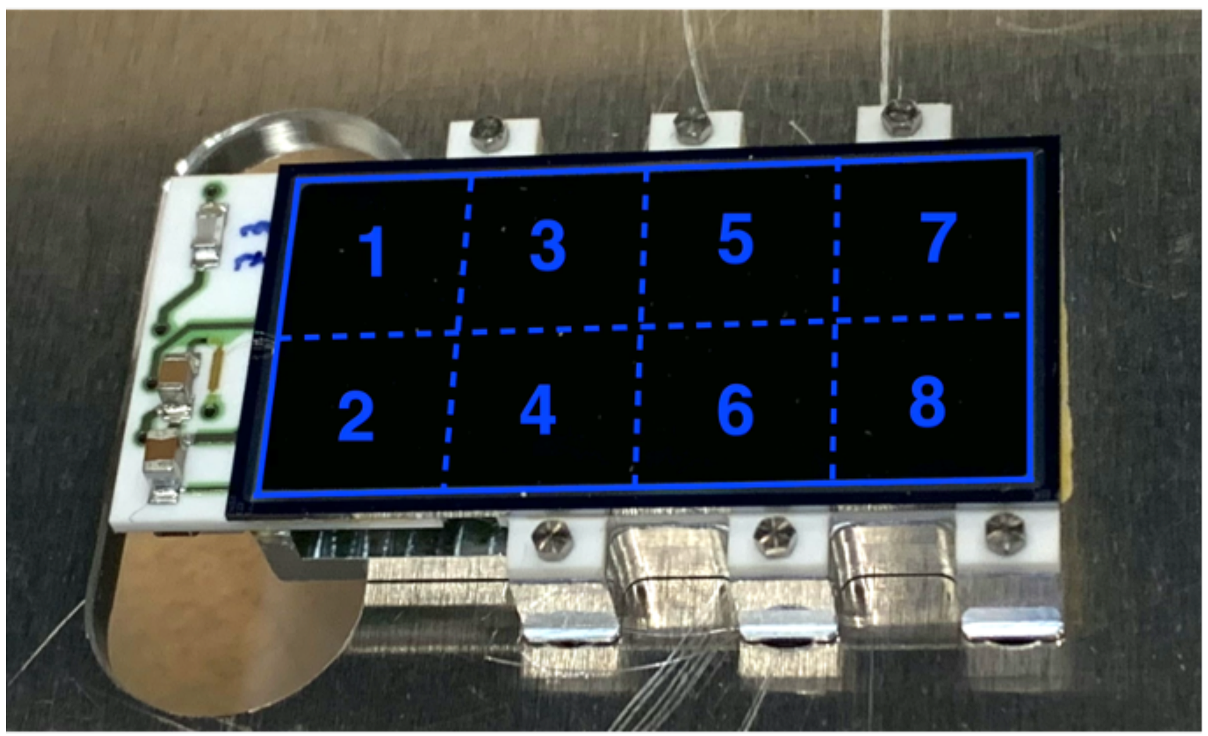

- High thermal conductive block: can be cooled down to (100÷150)K
- Preamplifier system in collaboration with Politecnico di Milano (PoliMi)
- CUBE: Metal-oxide semiconductor integrated charge sensing amplifier
- Small capacitance: lower rise time and independent from the detector's active area
- Large area detectors with a 500ns drift time at 140K

BACKUP

- e-h pairs separated through a reverse polarization field ("vertical drift")
- Second electric field superposed to transport the charges towards a collection anode ("horizontal drift")
- **"Gutter-like"** field configuration is achieved for the charge collection

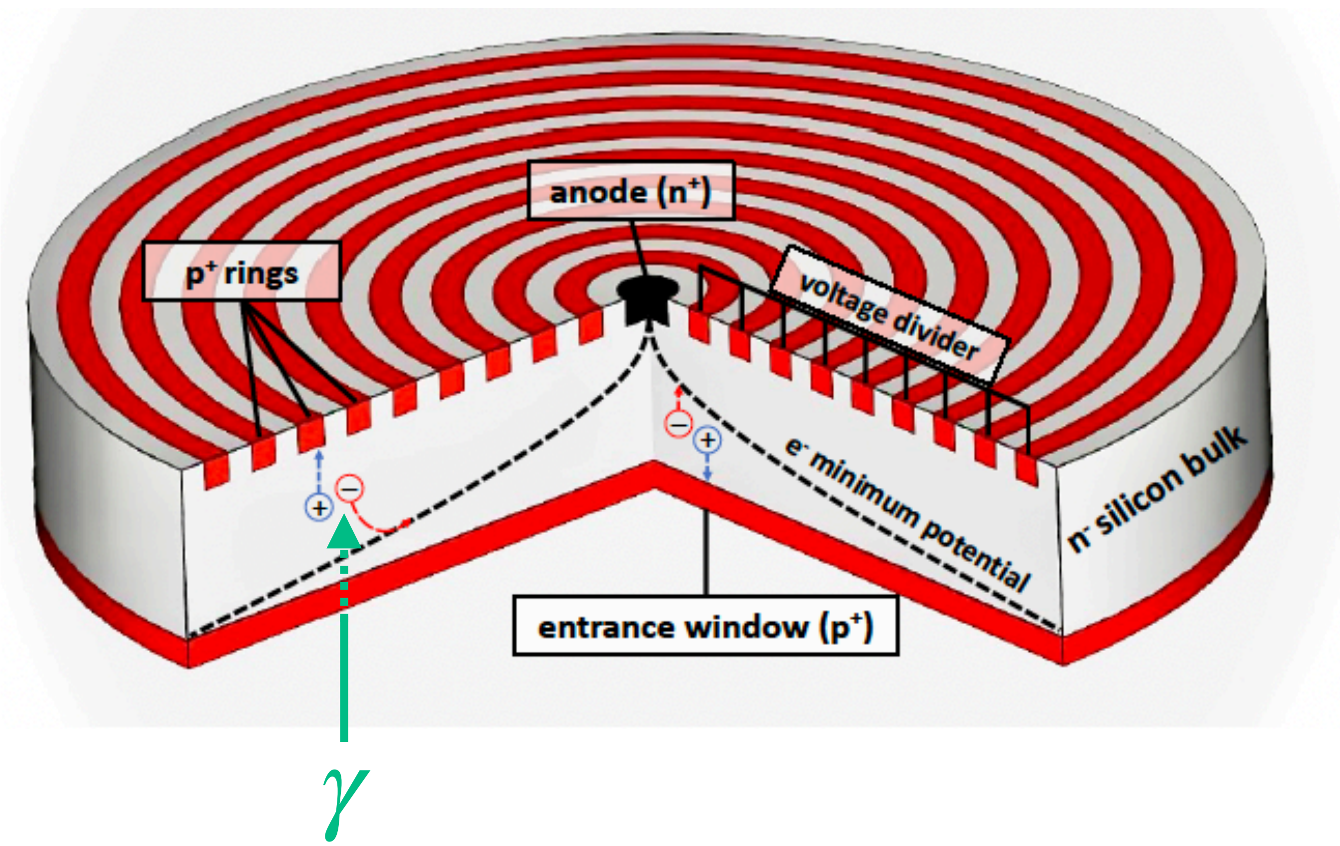

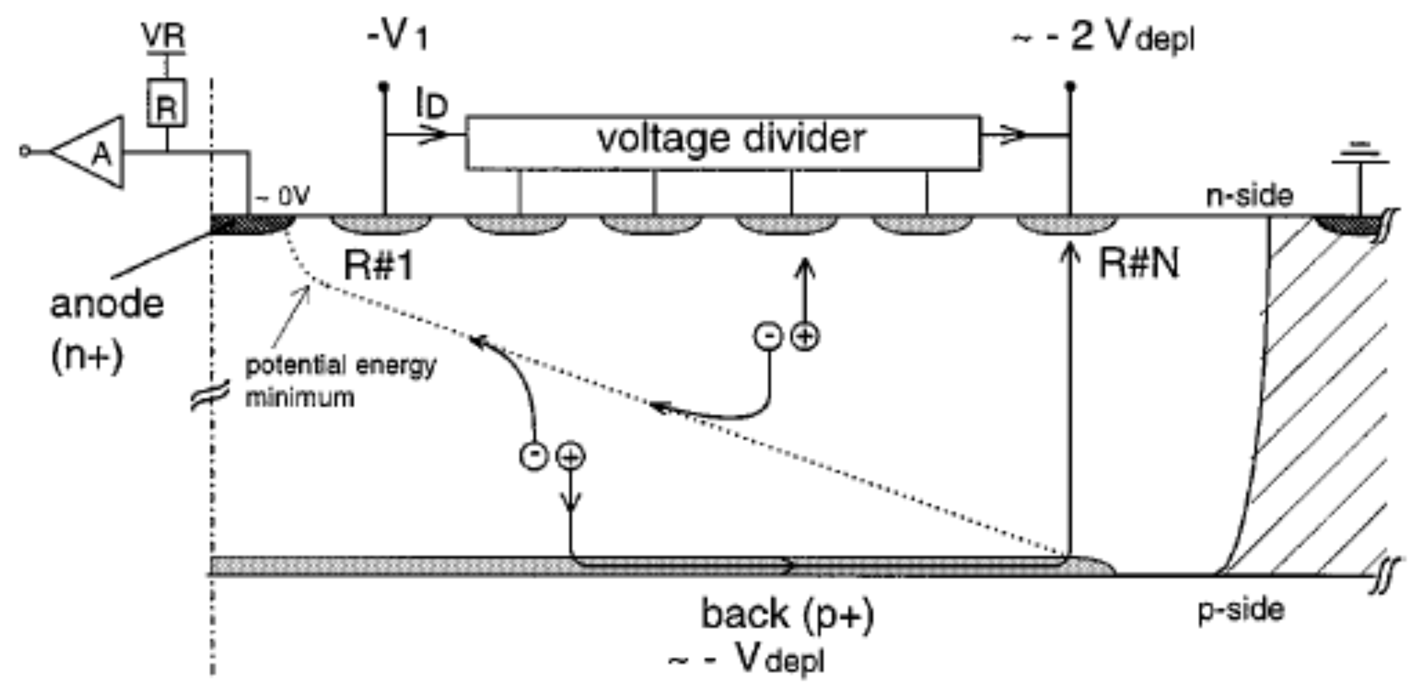

BACKUP

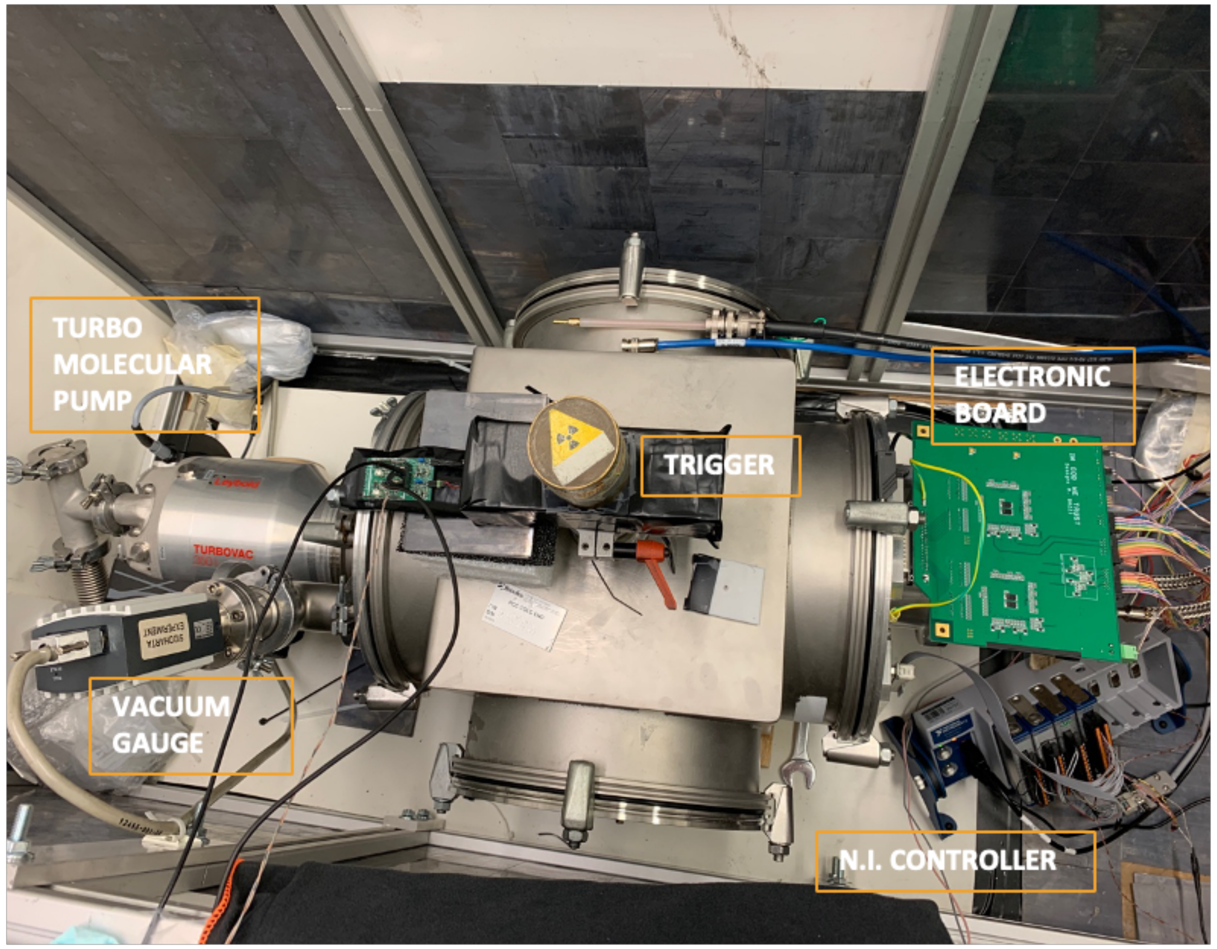
TURBO MOLECULAR PUMP
ELECTRONIC BOARD
TRIGGER
VACUUM GAUGE
N.I. CONTROLLER

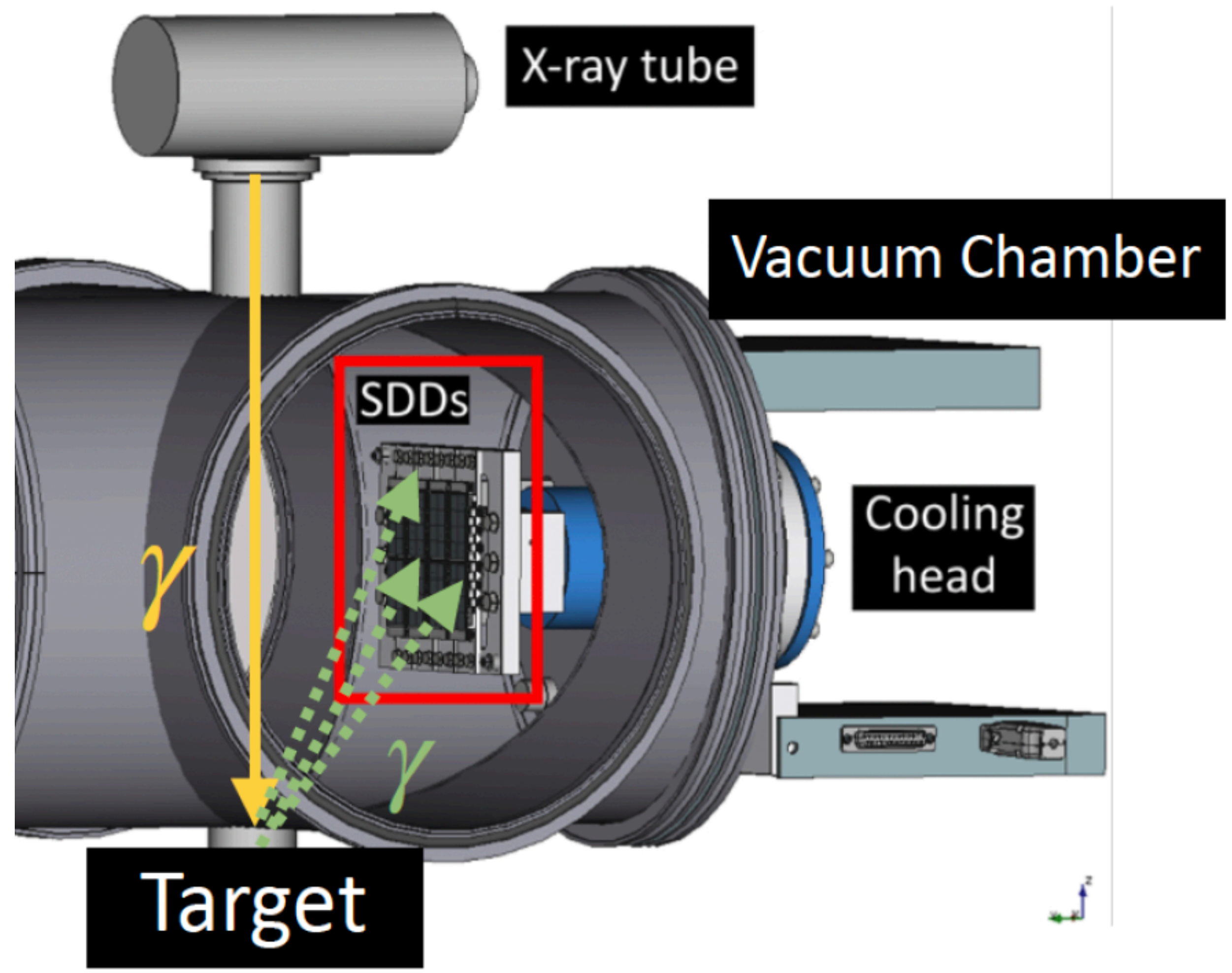
X-ray tube
Vacuum Chamber
SDDs
Cooling head
γ
γ
Target

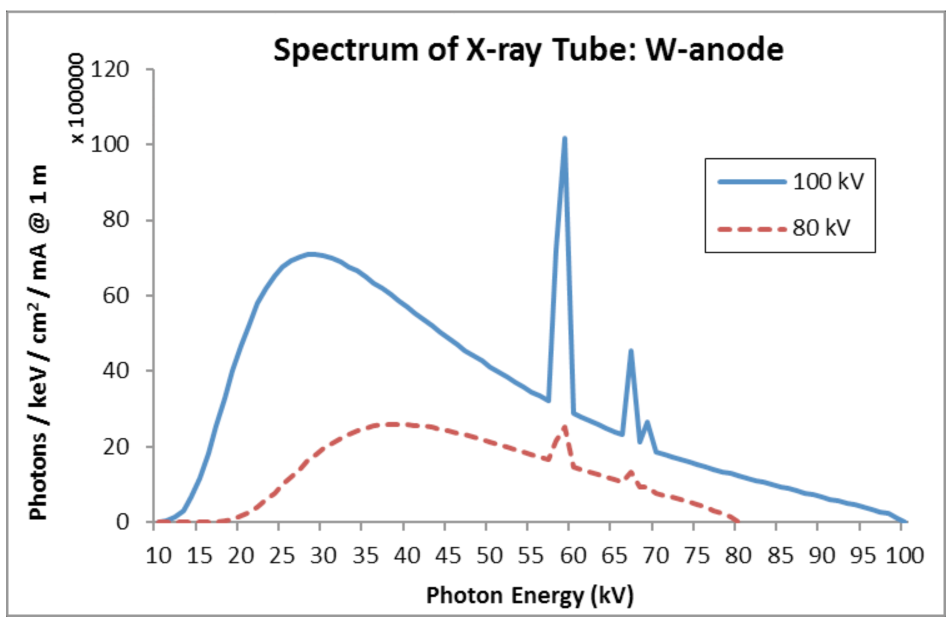
Spectrum of X-ray Tube: W-anode
x 100000
Photons / keV / cm² / mA @ 1 m
120
100
80
60
40
20
0
100 kV
80 kV
10 15 20 25 30 35 40 45 50 55 60 65 70 75 80 85 90 95 100
Photon Energy (kV)

BACKUP

- The energy response function of the SDD exhibits two main contributions:
    1. A Gaussian curve for every peak
    2. A Tail function accounting for the low energy component due to incomplete charge collection and e-h recombination
- A linear background has been taken into account
- A Peakfinder has been implemented using ROOT C++

$$T(x) = A_T \cdot e^{\frac{x-x_0}{\beta\sigma}+\frac{1}{2\beta^2}} \cdot erfc\left(\frac{x-x_0}{\sqrt{2}\sigma} + \frac{1}{\sqrt{2}\beta}\right)$$

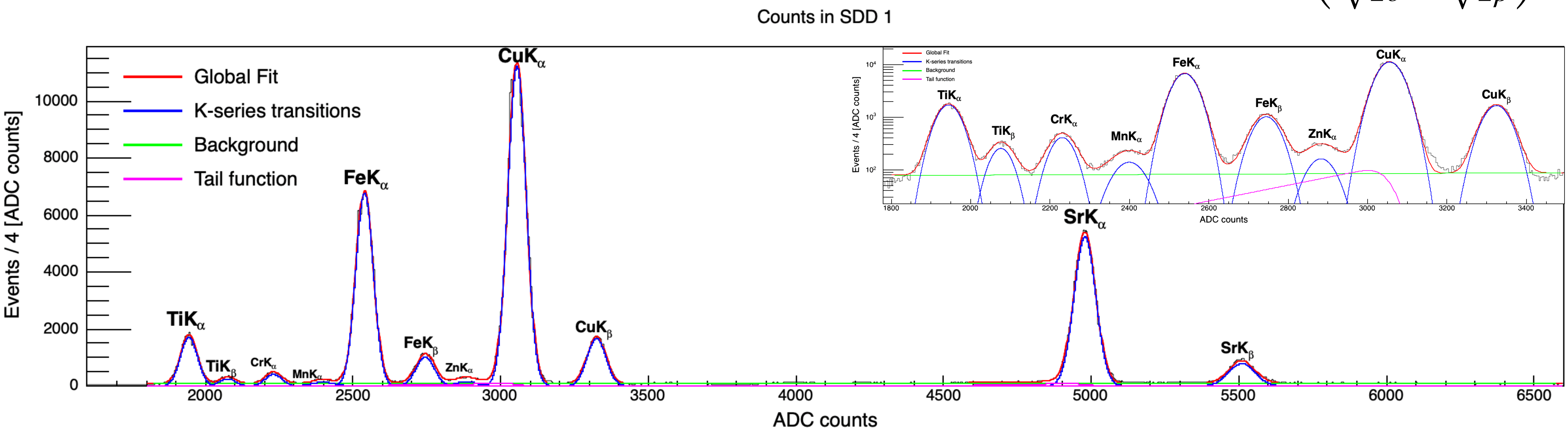

BACKUP

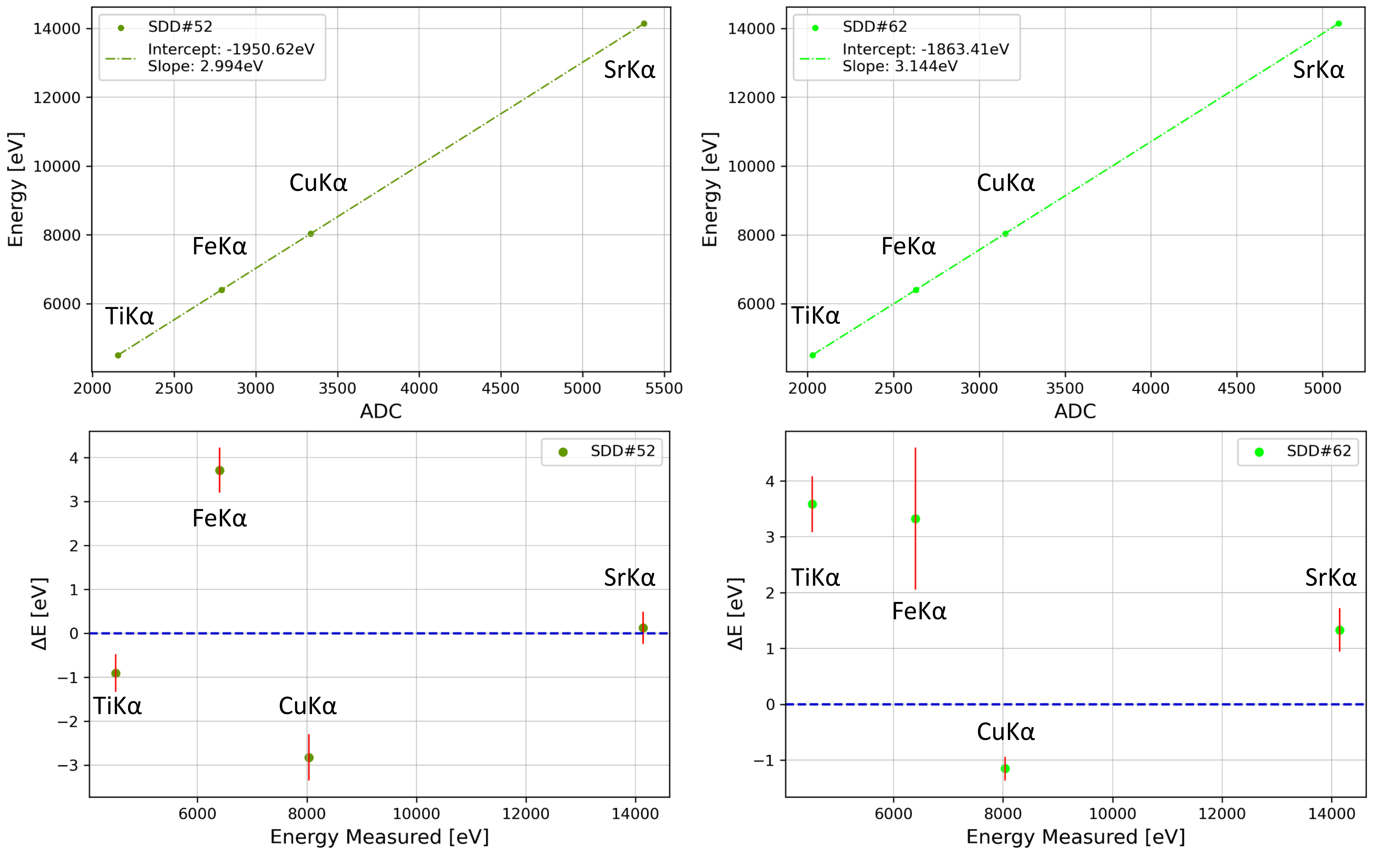
SDD#52
Intercept: -1950.62eV
Slope: 2.994eV
SrKα
CuKα
FeKα
TiKα
Energy [eV]
ADC
SDD#62
Intercept: -1863.41eV
Slope: 3.144eV
ΔE [eV]
Energy Measured [eV]

BACKUP

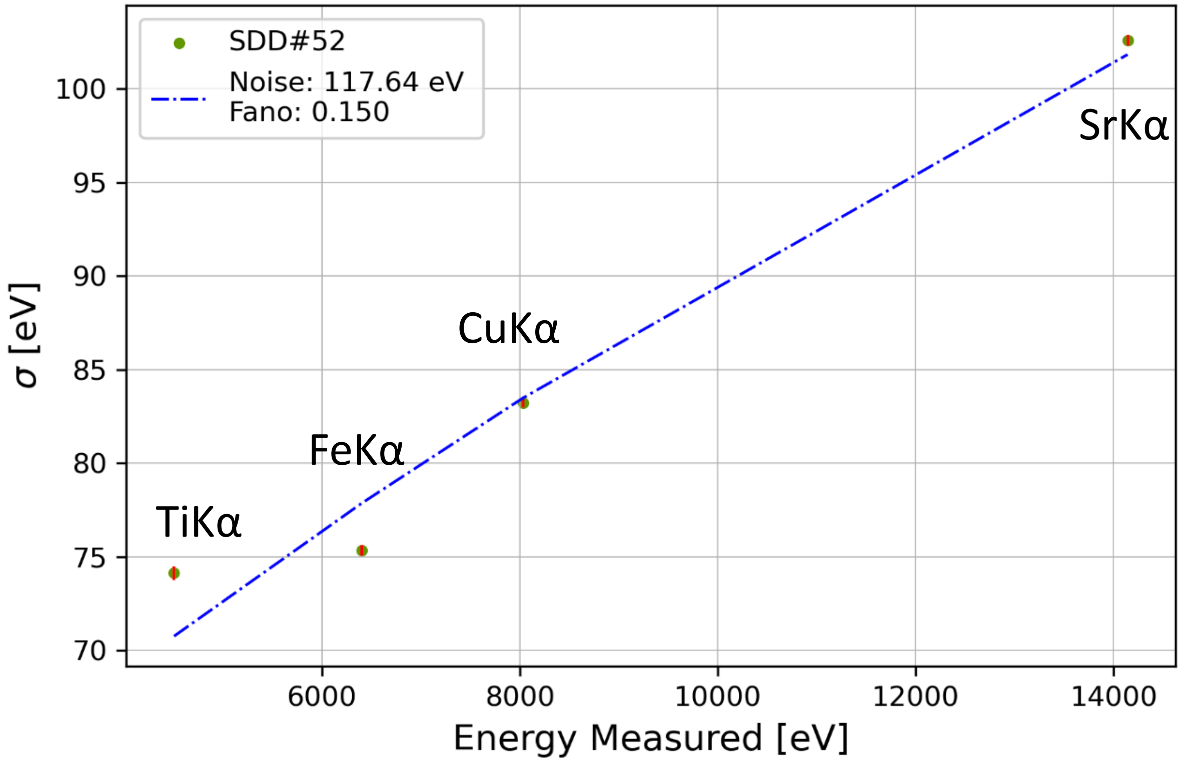

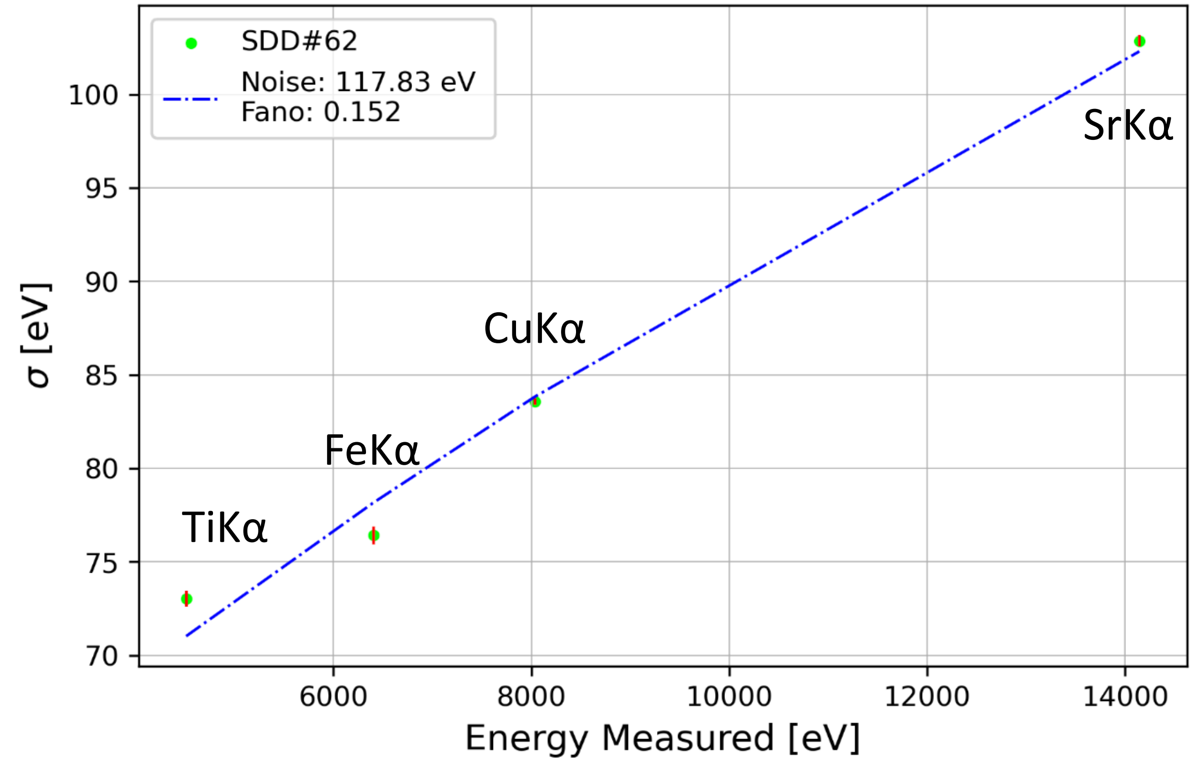

$$\sigma = \sqrt{FF \cdot \varepsilon \cdot E + \left(\frac{Noise}{2.35}\right)^2}$$

FWHM = (193 ± 1.5) eV (at 6.4keV)

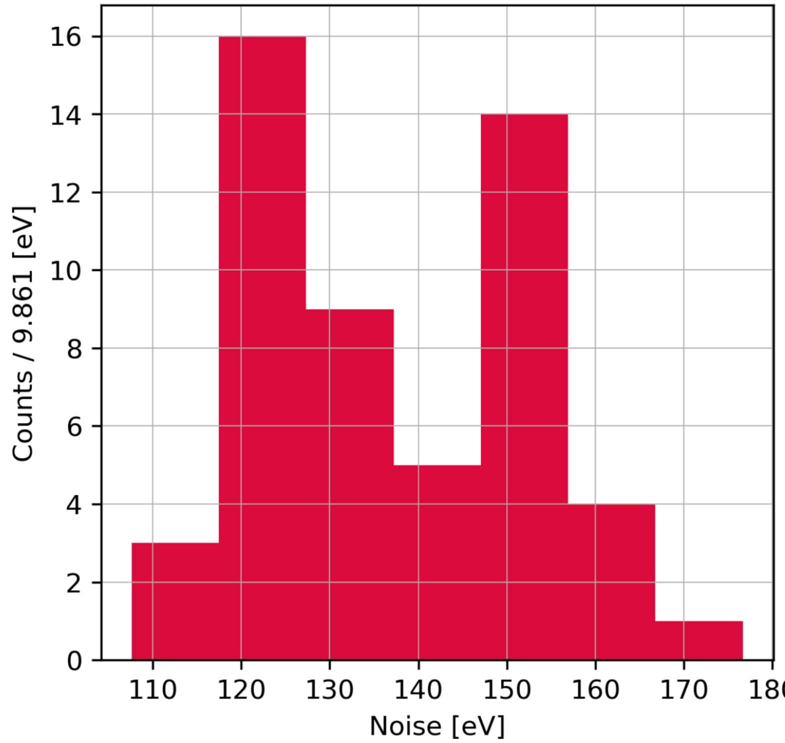

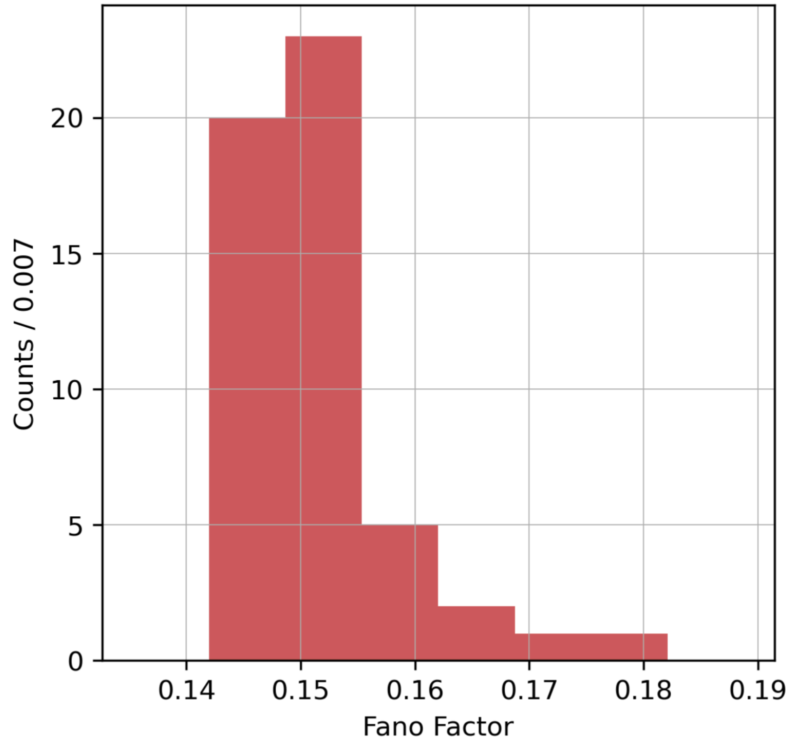

BACKUP

- Calibration of the SDDs system performed with two X-Ray tubes and a ^{55}Fe source
- 384 SDDs divided into 6 buses (64 SDDs each), 321 working SDDs analysed
- Sum of all the calibrated spectra to extract the resolution of the apparatus and the calibration error

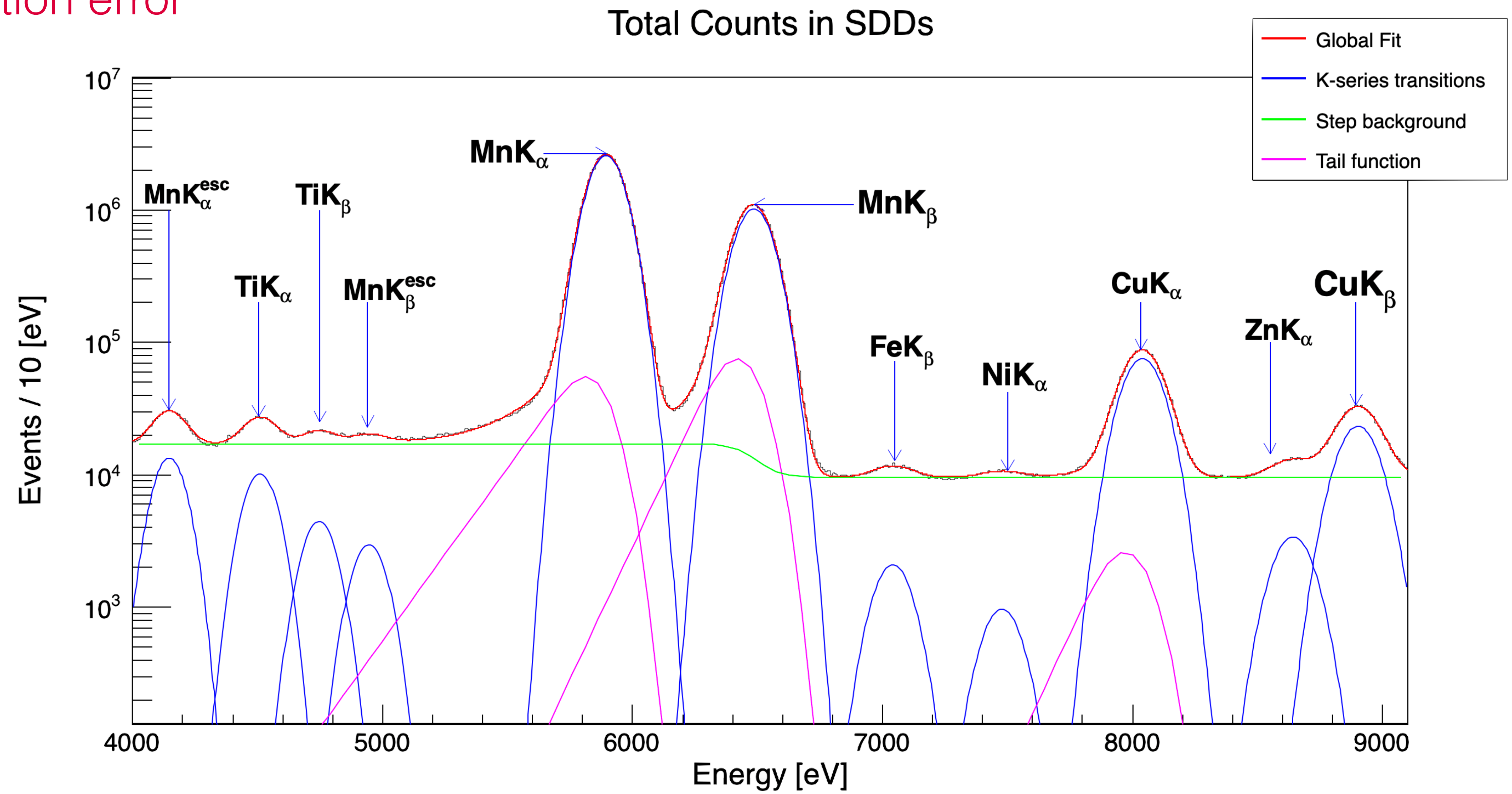

BACKUP

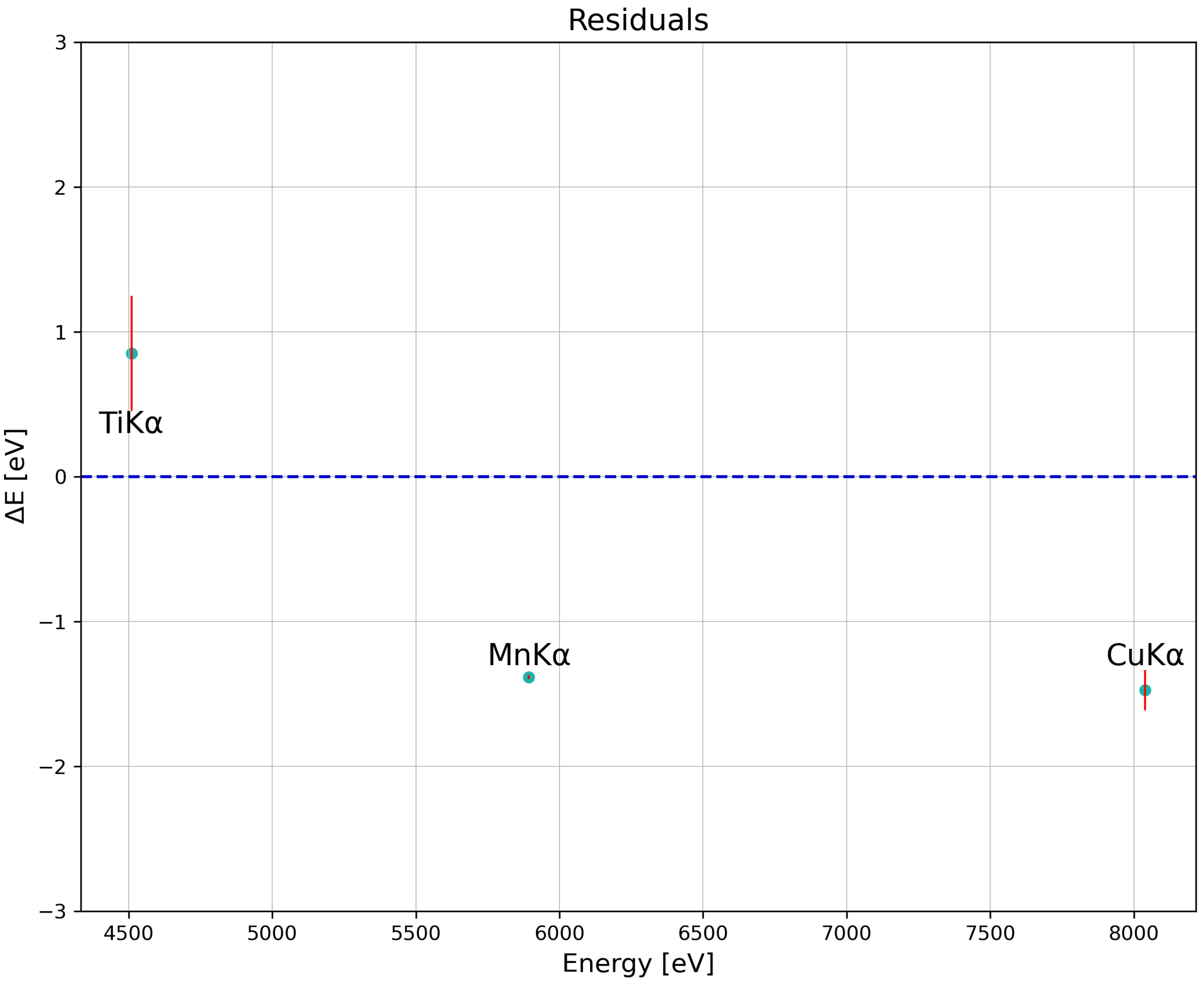

Calibration error ~ 1.5 eV at ~ 6 keV

FWHM $= (170.97 \pm 0.69)$ eV at ~ 6 keV

BACKUP

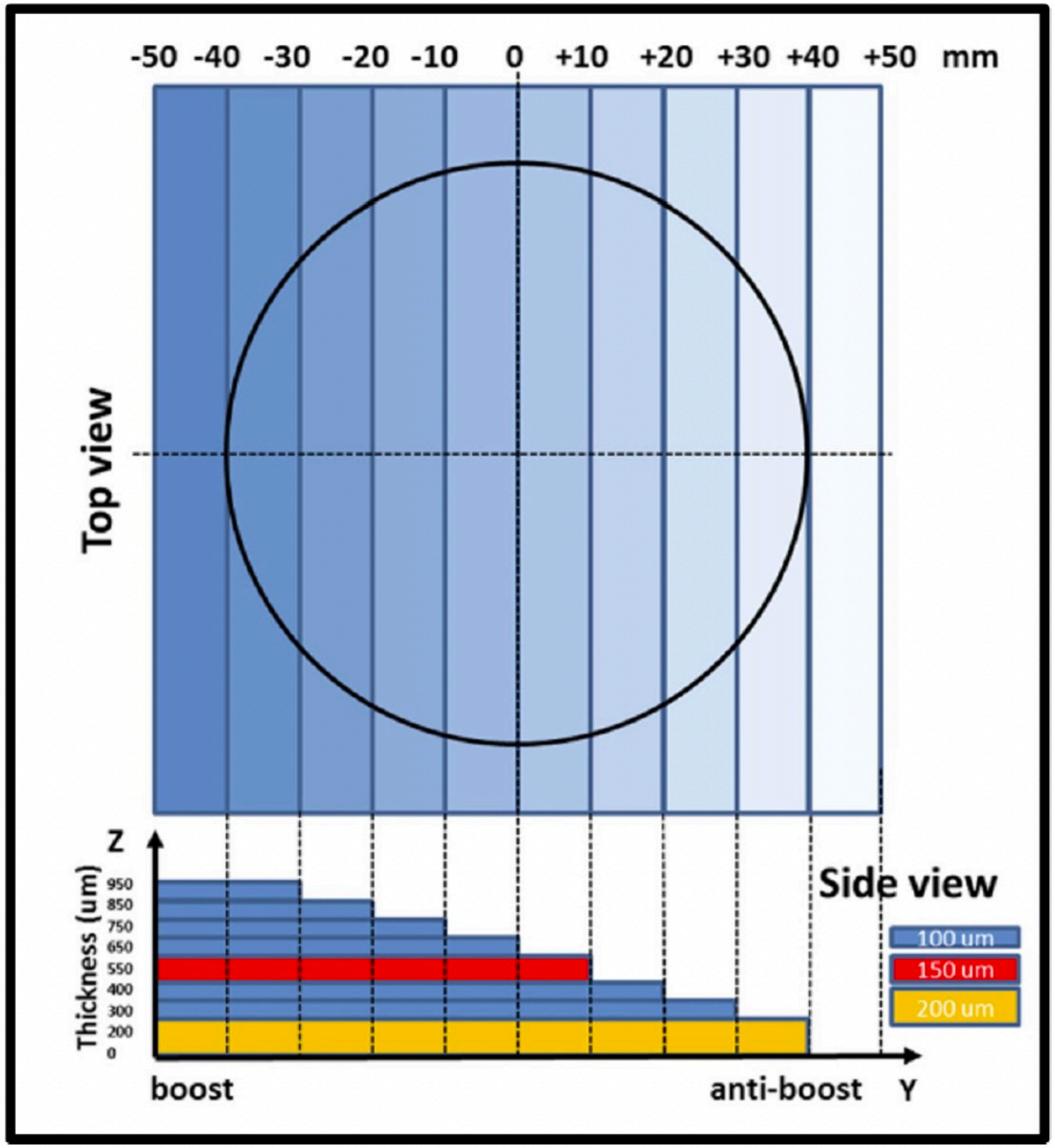

- Boost of the kaons towards the center of the collider
- Step-wise mylar degrader to obtain a uniform stopping distribution inside the target cell
- Eight mylar strips with thickness varying from 100μm-200μm
- Overall thickness ranges from 200μm-950μm
- MC simulations + Experimental fine tuning to optimise the shape and thickness

BACKUP

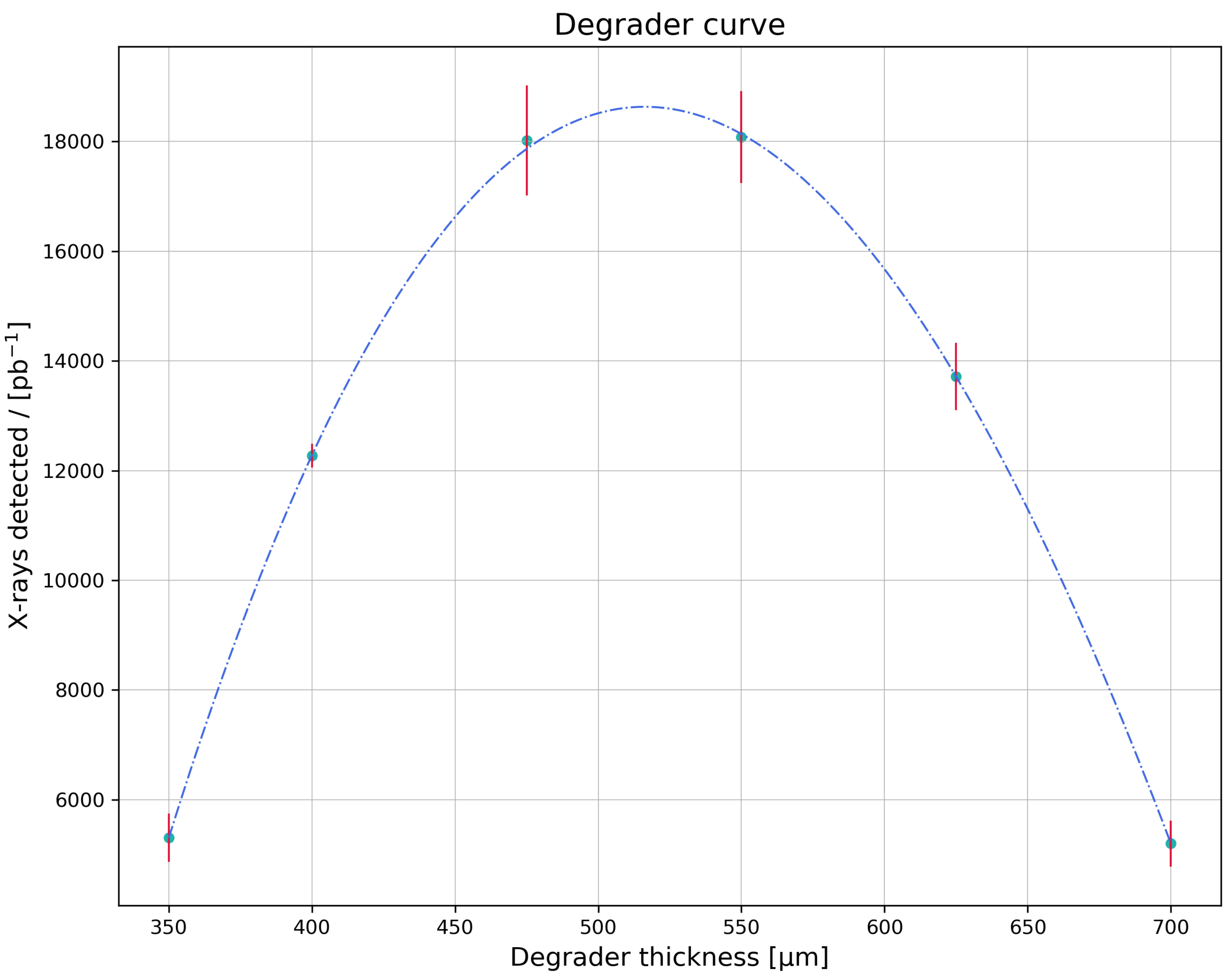

- Six different degrader thickness: 350μm, 400μm, 475μm, 550μm, 625μm and 700μm in the middle
- Number of kaonic helium-4 L_α $(3d \rightarrow 2p)$ events measured, normalised to the integrated luminosity of each data taking
- Optimal thickness of ~516μm
- 150μm-160μm difference results in a reduction of a factor ~3 in the X-Ray yield
- **Crucial step** in the view of the kaonic deuterium measurement

BACKUP

ε_{2p} (eV)	Ref.
-41±33	Wiegand *et al.* [19]
-35±12	Batty *et al.* [20]
-50±12	Baird *et al.* [21]
-43±8	Average of the above [21, 22]
+2±2(stat)±2(syst)	Okada *et al.* [25]
0±6(stat)±2(syst)	Bazzi *et al.* [26]

Table 1.2. Summary of the shift of the $3d \rightarrow 2p$ kaonic helium transition.

[19] Wiegand, C. E. & Pehl, R. H. Measurement of kaonic X-rays from He-4. *Physical Review Letters* **27**, 1410 (1971).

[20] Batty, C. *et al.* Measurement of kaonic and pionic X-rays from liquid helium. *Nuclear Physics A* **326**, 455–462 (1979).

[21] Baird, S. *et al.* Measurements on exotic atoms of helium. *Nuclear Physics A* **392**, 297–310 (1983).

[22] Batty, C. Light kaonic and antiprotonic atoms. *Nuclear Physics A* **508**, 89–98 (1990).

[25] Okada, S. *et al.* Precision measurement of the 3d→ 2p x-ray energy in kaonic 4He. *Physics Letters B* **653**, 387–391 (2007).

[26] Bazzi, M. *et al.* Kaonic helium-4 x-ray measurement in SIDDHARTA. *Physics Letters B* **681**, 310–314 (2009).

BACKUP

QED predicted values

Transition	Energy [eV]	Transition	Energy [eV]
K-^{4}He M_δ	4213.3	Ti K_α	4500.9
K-^{4}He M_η	4696.6	Ti K_β	4932
K-^{4}He L_α	6463.3	K-C $6 \to 5$	5544.9
K-^{4}He L_β	8721.6	K-O $7 \to 6$	6006.8
K-^{4}He L_γ	9766.6	K-N $6 \to 5$	7595.4
K-^{4}He L_δ	10334.3	K-C $7 \to 5$	8885.8
K-^{4}He L_ϵ	10676.5	K-O $6 \to 5$	9968.7
K-^{4}He L_ζ	10898.7	K-C $5 \to 4$	10216.5
K-^{4}He L_η	11050.9	-	-
K-^{4}He L_θ	11159.9	-	-

Measured values

Transition	Energy [eV]
K-^{4}He M_δ	4192 ± 16
Ti K_α	4501.7 ± 6.1
K-^{4}He M_η	4710 ± 22
Ti K_β	4926 ± 18
K-C $6 \to 5$	5546.5 ± 8.0
K-O $7 \to 6$	6025 ± 17
K-^{4}He L_α	6461.3 ± 1.2
K-N $6 \to 5$	7578 ± 39
K-C $7 \to 5$	8917 ± 27
K-O $6 \to 5$	9978 ± 11
K-C $5 \to 4$	10212.6 ± 6.6